



NRL/MR/7430--02-8274

NRL-APL Grain Size Algorithm Upgrade

KEVIN B. BRIGGS

*Seafloor Sciences Branch
Marine Geosciences Division*

DARRELL R. JACKSON

K. Y. MORAVAN

*Applied Physics Laboratory
University of Washington
Seattle, WA*

June 28, 2002

Approved for public release; distribution is unlimited.

REPORT DOCUMENTATION PAGE				Form Approved OMB No. 0704-0188	
Public reporting burden for this collection of information is estimated to average 1 hour per response, including the time for reviewing instructions, searching existing data sources, gathering and maintaining the data needed, and completing and reviewing this collection of information. Send comments regarding this burden estimate or any other aspect of this collection of information, including suggestions for reducing this burden to Department of Defense, Washington Headquarters Services, Directorate for Information Operations and Reports (0704-0188), 1215 Jefferson Davis Highway, Suite 1204, Arlington, VA 22202-4302. Respondents should be aware that notwithstanding any other provision of law, no person shall be subject to any penalty for failing to comply with a collection of information if it does not display a currently valid OMB control number. PLEASE DO NOT RETURN YOUR FORM TO THE ABOVE ADDRESS.					
1. REPORT DATE (DD-MM-YYYY) June 28, 2002		2. REPORT TYPE Memorandum		3. DATES COVERED (From - To)	
4. TITLE AND SUBTITLE NRL-APL Grain Size Algorithm Upgrade				5a. CONTRACT NUMBER N0003901WXDF202	
				5b. GRANT NUMBER	
				5c. PROGRAM ELEMENT NUMBER 63207N	
6. AUTHOR(S) Kevin B. Briggs, Darrell R. Jackson,* and K.Y. Moravan*				5d. PROJECT NUMBER 74-7076-A1	
				5e. TASK NUMBER	
				5f. WORK UNIT NUMBER 71-7076-00	
7. PERFORMING ORGANIZATION NAME(S) AND ADDRESS(ES) Naval Research Laboratory Marine Geoscience Division Stennis Space Center, MS 39529-5004				8. PERFORMING ORGANIZATION REPORT NUMBER NRL/MR/7430--02-8274	
9. SPONSORING / MONITORING AGENCY NAME(S) AND ADDRESS(ES) Space and Naval Warfare Systems Command Kim Koehler PMW 155-12A Meteorology and Oceanography Systems San Diego, CA 92110-3127				10. SPONSOR / MONITOR'S ACRONYM(S) SPAWAR	
				11. SPONSOR / MONITOR'S REPORT NUMBER(S)	
12. DISTRIBUTION / AVAILABILITY STATEMENT Approved for public release; distribution unlimited.					
13. SUPPLEMENTARY NOTES *Applied Physics Laboratory, University of Washington, Seattle, WA 98105					
14. ABSTRACT This upgrade was designed to improve upon older algorithms used to infer input geoacoustic parameters for high-frequency acoustic models from sediment grain size. These older algorithms were based on a limited data set and were developed by adjusting acoustic model-data fits rather than by statistical regression. The upgrade has two components. The regression analysis of sediment grain size and geoacoustic properties was performed by NRL and the determination of accuracy of acoustic backscatter predictions was performed by APL-UW. The geoacoustic properties/sediment grain size relationships produced a new algorithm connecting acoustic model parameters with the parameters of the MIW (Mine Warfare) sediment database.					
15. SUBJECT TERMS Backscattering, Grain size, Regression analysis					
16. SECURITY CLASSIFICATION OF:			17. LIMITATION OF ABSTRACT UL	18. NUMBER OF PAGES 38	19a. NAME OF RESPONSIBLE PERSON Kevin Briggs
a. REPORT Unclassified	b. ABSTRACT Unclassified	c. THIS PAGE Unclassified			19b. TELEPHONE NUMBER (include area code) (206) 543-1328

CONTENTS

ABSTRACT	1
BACKGROUND	1
METHODS	2
NRL Sediment Database Collation	2
APL-UW Acoustic Database Collation	2
RESULTS	2
Geoacoustic Data	2
Regression Analysis	3
High-Frequency Bottom Backscattering Model Predictions	5
DISCUSSION AND SUMMARY	5
ACKNOWLEDGMENTS	6
REFERENCES	6
APPENDIX 1	17

NRL-APL Grain Size Algorithm Upgrade

Abstract

This upgrade was designed to improve upon older algorithms used to infer input geoacoustic parameters for high-frequency acoustic models from sediment grain size. These older algorithms were based on a limited data set and were developed by adjusting acoustic model-data fits rather than by statistical regression. The upgrade has two components. The regression analysis of sediment grain size and geoacoustic properties was performed by NRL and the determination of accuracy of acoustic backscatter predictions was performed by APL-UW. The geoacoustic properties/sediment grain size relationships produced a new algorithm connecting acoustic model parameters with the parameters of the MIW (Mine Warfare) sediment database.

NRL collated available geoacoustic data and made regression fits to grain size and related grain size parameters to descriptors used in the MIW database. The sediment volume scattering parameter, unlike all other parameters, was determined from acoustic model fits rather than from core data. Error estimates for the empirical fitting functions are given as the coefficient of determination, which denotes the proportion of variability in the predicted parameter that is explained by the variability in the predictor parameter (usually mean grain size).

APL-UW collated all available backscatter data from the areas where geoacoustic data were collected, ran the OAML high-frequency bottom backscattering model using NRL inputs, and compared the results with data. Acoustic model error estimates were determined from these comparisons. The new algorithm represents up-to-date geoacoustic data more faithfully than the older algorithms. The older algorithms, however, provide a somewhat better fit to the acoustic data, in part because they were developed by fitting a substantial portion of the acoustic data used here in response to the disparity between measurement and prediction. It is recommended that a second set of regressions be performed to optimize the acoustic fit with some compromise in accuracy of the geoacoustic fit.

Background

Since the publication of APL-UW-TR-9407 in 1994 there have been a number of high-frequency acoustic experiments conducted in shallow-water environments in diverse sediments. During the same time period more environmental and acoustic data have been processed by the Naval Research Laboratory (NRL) and Applied Physics Laboratory, University of Washington (APL-UW), providing new and more refined interpretations of acoustic-sea floor interactions. Moreover, the empirical relationships among geoacoustic properties and grain size relied on by APL-UW-TR-9407 were derived from data of Hamilton and Bachman (1982) that were not exclusively collected from the uppermost sediments from continental shelves. The NRL and APL-UW data were collected only from shallow-water environments (10-300 m water depth) where co-located sediment and acoustic measurements were made. These new data and subsequent interpretations were re-examined in light of the needs of the Naval Oceanographic Office to apply the bottom backscattering model from the Oceanographic and Atmospheric Master Library (OAML) to the diversity of sediment types encountered in shallow-water MCM operations around the world.

There are 23 sediment types listed in the table relating bottom backscattering model parameters to sediment type in Table 2 of Section IV of APL-UW-TR-9407 (1994). It is difficult to reconcile the 200+ sediment types listed in the MIW sediment database with the 23 types listed in the table. Furthermore, values for parameters such as the spectral exponent (γ) and volume scattering (σ_2) are fitted to the bottom backscattering model with only minimal range of variation (one and two possible values, respectively). These sediment surface and volume scattering parameters exhibit a wider range of variation in nature than is allowed by the table in APL-UW-TR-9407. Hence, an effort was undertaken to link the model inputs directly to empirically derived algorithms based on grain size rather than with the scenarios established in Table 2 of APL-UW-TR-9407.

Methods

NRL Sediment Database Collation

Values of sediment compressional wave velocity (sound speed) and attenuation were measured at 400 kHz in cores collected by divers or from box cores from 23 different sites around the world (all but two of the sites were located on the continental shelf of the U.S.). Measurements were made with a pulse technique on intact, freshly collected, relatively undisturbed samples to ensure high-quality, consistent data for analysis. These same core samples were later subjected to laboratory analyses for porosity, density and grain size distribution, thus providing a direct, physical correspondence among all measurements. Sediment surface roughness was measured photogrammetrically at almost every site (Briggs, 1989). Measurements of roughness were made at the same time as the acoustic backscattering measurements in every instance but one. Relative height measurements of the sediment surface were used to estimate roughness power spectra, from which regression parameters of slope and intercept were derived.

APL-UW Acoustic Database Collation

Acoustic backscattering data were collected from either towed or bottom-mounted sonars at frequencies of 20, 25, 35 or 40 kHz. Most of these data were collected by APL-UW, with the remainder collected by Applied Research Laboratories-University of Texas, Naval Undersea Warfare Command, or NRL. Data were collected and a variety of grazing angles and azimuths, but were averaged over all azimuths for comparison purposes. Anisotropy in surface features that might cause azimuthal-dependent scattering occurred at only four of the 23 sites and actual azimuthal dependence in scattering from ripples was not statistically observable.

Results

Geoacoustic Data

NRL collated the parameters of sediment sound speed (V_p), sediment sound speed ratio (V_p/R), sediment sound speed variance (σ^2-V), sediment sound attenuation (dB/m), mean grain size in ϕ units (M_z), porosity (β), bulk density (ρ), density ratio (ρ_Ratio), density variance ($\sigma^2-\rho$), density correlation length (l_c), sound speed attenuation normalized to frequency (k), sediment

type, roughness spectral exponent (γ_1), and roughness spectral intercept (w_1) for the 23 sites in Table 1. Parameters of sediment sound speed ratio and density ratio are defined as ratios of the value in the sediment to the value in the overlying water. Table 1 is composed of average values for the parameters from entire cores; the parameter values in Table 2 are restricted to the top 2 cm of the cores. The 0-2-cm increment of the core samples represents the values that might be measured from grab samples and the values that determine the acoustic impedance for highly reflective sea floors, which are generally coarse-grained. The 23 sites are arranged in order of decreasing mean grain size (increasing values of ϕ), from coarse shell hash to silty clay. Bottom roughness parameters are incomplete because the roughness measurements from the six sites in the approaches to the Strait of Juan de Fuca (JDF) have not been processed yet.

Regression Analysis

All of the contents of the database (over 4800 individual sediment depth increments) were used to generate Table 1. From the mean parameters of Tables 1 and 2, we can make predictions of acoustic backscattering at each of the 23 sites. Also from the entire database we can construct empirical relationships among the individual parameters via regression analysis. Examples of regressions derived from the entire database are presented in Figs. 1 and 2. Because the datasets from each site include systematic measurements downcore for each parameter and, hence, vertical gradients inherent in surficial sediment properties, serial correlation between the regressed parameters has been introduced to the analysis. To avoid the inaccuracy of generating predictions based on serially correlated data, we averaged the parameters over each core, thus eliminating the surficial gradients apparent in the measured data. The averaging resulted in a database consisting of 137 cores representing 23 sites from which all subsequent regression equations are derived.

In order to link the geoacoustic properties to grain size parameters, Table 3 is provided. In addition, information on site locations is referred to in this table as well as Table 3A. Parameters of percentage by weight of gravel, sand, silt, and clay and sorting are listed for the 23 sites. Sorting is a graphic measure of the dispersion of size classes around the mean grain size (graphic standard deviation). The σ_2 parameter is a fitted parameter indicative of sediment volume scattering chosen to adjust the level of predicted backscatter to the level of the measured intensity. This parameter is used in the model presented in APL-UW-TR-9407 in lieu of the sound speed and density variance and density correlation length parameters (Table 1) used in the perturbation theory approach to sediment volume scattering (Jackson et al., 1996). Mean values are slightly different from Table 1 because (1) we restricted the database exclusively to measurements that were co-located at each depth and (2) core length varied both within and among sites. Processing the data this way also reduced the variance of the individual parameters at each site.

Using grain size parameters of mean grain size (M_z), sorting (srt), percent gravel (gr), sand (sa), silt (si), and clay (cl) to predict sound speed ratio (VpR), bulk density (ρ), normalized attenuation (k), roughness spectral exponent (γ_1), roughness spectral intercept (w_1), and volume scattering parameter (σ_2) we derived the following empirical relationships, which may be multiple linear, non-linear, or piecewise non-linear regressions:

$VpR = 1.1807 - 0.0187 \cdot M_z - 0.0142 \cdot srt - 0.00195 \cdot gr$	$r^2 = 0.95$
<i>or</i>	
$VpR (0-7.74) = 1.086 + 0.057 \cdot M_z - 0.0201 \cdot M_z^2 + 0.0014 \cdot M_z^3$	$r^2 = 0.88$
$VpR (>7.75) = 1.549 - 0.135 \cdot M_z + 0.008 \cdot M_z^2$	$r^2 = 0.42$
$\rho = -378.251 + 1032.0 \cdot VpR - 934.48 \cdot VpR^2 + 282.31 \cdot VpR^3$	$r^2 = 0.97$
$k (0-3.84 \phi) = 0.437 + 0.09 \cdot M_z - 0.03 \cdot M_z^2$	$r^2 = 0.07$
$k (3.85-5.1 \phi) = 0.476 \cdot M_z - 1.464$	$r^2 = 0.70$
$k (5.11-9.5 \phi) = 4.026 \cdot e^{(-0.279 \cdot M_z)}$	$r^2 = 0.61$
$\gamma_1 = 0.07 \cdot cl + 0.06 \cdot si + 0.06 \cdot sa - 3.197$	$r^2 = 0.52$
<i>or</i>	
$\gamma_1 = 0.12 \cdot M_z + 2.00$	$r^2 = 0.35$
$w_1 (0-1.8 \phi) = 0.00718 - 0.00398 \cdot M_z$	$r^2 = 0.54$
$w_1 (1.81-4.59 \phi) = 0.00032 \cdot M_z - 0.00056$	$r^2 = 0.46$
$w_1 (4.6-9.5 \phi) = 7.46 \cdot M_z^{-5.91}$	$r^2 = 0.76$
$\sigma_2 = 0.000059 \cdot M_z^{1.4}$	$r^2 = 0.28$

The coefficient of determination (r^2), or the proportion of the variation in the predicted parameter explained by the variation in the parameter used as a predictor, is displayed to the right of each regression. Coefficients of determination are disappointingly low for some of the relationships. However, values for r^2 are very good for two of the most significant determinants of bottom scattering: sound speed and density ratio (density ratio may be calculated from bulk density by dividing by the density of seawater, or 1.023). Accurate prediction of sound attenuation (k) in coarse sediment (M_z less than 3.85ϕ) was difficult due to scattering of the 400-kHz sound by the coarse particles. Despite the low r^2 value for the coarsest grain sizes, we advocate the use of the piecewise regression in Fig. 3 based on the empirical relationship previously derived by Hamilton and Bachman (1982). Sediment type is a particularly weak predictor of the roughness spectral exponent (γ_1), due to high variability in power spectral slopes that is a function of bioturbation and storms, which have a definite temporal dependence. The roughness spectral intercept (w_1), which indicates the relative strength of high-frequency spatial roughness elements, exhibits grain-size-dependent behavior, and may be related to the mobility of sediment. That is, there is a lack of high-frequency roughness (low w_1 values) at intermediate mean grain diameters offering the least resistance to entrainment by currents. Furthermore, sea floors composed of very small particles (muds) would exhibit little high-frequency spatial roughness due to cohesion. Thus, one would expect minima in the predictions of the roughness spectral intercept at intermediate and fine grain sizes as is found in the empirical relationship above (Fig. 4). The accuracy of predicting the sediment volume scattering parameter (σ_2) from mean grain size is poor ($r^2 = 0.28$) because the σ_2 parameter is a fitted parameter that incorporates all the unexplained uncertainties that affect scattering predictions from environmental variables.

High-Frequency Bottom Backscattering Model Predictions

APL-UW collated the available backscatter data collected during the field experiments that were conducted concomitantly with the 23 environmental data collections in Tables 1-3. The high-frequency bottom backscattering model from the Oceanographic and Atmospheric Master Library (OAML) was run using NRL inputs and comparisons were made with the collated acoustic data. Root-mean-squared error of the model data fit (with both model and data values expressed in dB) was also calculated. Typically, the backscatter data cover grazing angles between 10 to 40 degrees. We chose four sources of input parameters to test the model: regressions on mean grain size (M_z), multiple regressions on grain size parameters (M_z , srt , gr , sa , si , cl), average values from the surficial (0-2 cm) measurements in Table 2, and the parameterization results from APL-UW-TR-9407 based on surficial grain size (M_z).

We were unable to make comparisons with the acoustic data collected by ARL-UT because of differences in the nature of these data. First, the ARL-UT measurements focused on very low grazing angles (typically below 10°) and are disjoint for the other data sets in this respect. Second, the data were interpreted in terms of a Lambert-Law fit to single-ping scattering strength, while the other data sets were used to form multiple-ping intensity averages. It is certain that the former method is biased significantly lower than the latter, but the extent of this bias is difficult to estimate, in part because lower-angle data also suffer potentially from bias due to surface scattering. The remaining 18 comparisons are presented as Appendix 1. A summary of the model-data comparisons is given in Table 4; the fit was deemed “best” if it was within 2 dB of measured data and deemed “acceptable” if it was within 2-4 dB of measured data. Whereas the parameter values from APL-UW-TR-9407 provided the most accurate model predictions (“best” fit for seven of the 18 comparisons, “acceptable” fit for three of the 18), the model predictions provided by the new regressions for surficial values of parameters were nearly as accurate (“best” fit for three of the 18 comparisons, “acceptable” fit for six of the 18). Parameters predicted from the single and multiple regression equations gave good or acceptable model fits to data at only six of the 18 sites. Some acoustic data were not fit adequately using any one of the four sources of model inputs (MonPt, Tirr and JDF7). The root-mean-square error in dB between the model predictions and the measured data are given in Table 5.

Discussion and Summary

An attempt was made to update the empirical relationships between geoacoustic properties used as model parameters and sediment grain size in order to improve the accuracy of acoustic modeling. The regression equations presented here represent the latest database derived from continental shelf sediments where acoustic measurements were made. In principle, these data are superior to the algorithms in APL-UW-TR-9407, which were based on data compiled from deep-water ocean sedimentary provinces and unsupported with acoustic backscatter data. Our objective was to supplant the tabulated results in APL-UW-TR-9407 because of the incongruity between the 23 sediment types listed in 9407 and the 215 (plus) sediment types listed in the MIW database. Rather than ramifying the 23 sediment categories into 215+ sediment types, we advocate the use of grain size parameters available from standard core analysis to make predictions of bottom backscatter.

Although the older algorithms give better fits to the acoustic data than those developed here, this is because the older algorithms were produced by fitting *acoustic* data whereas the newer algorithms were produced by fitting *geoacoustic* data. In fact, the older algorithms employed several of the sites used here in determining prediction error, so the relatively good performance of the older algorithms is not surprising. It is likely that the acoustic fitting process partially corrected unknown deficiencies in the acoustic models. The newer algorithms employ a larger database and should be more robust with respect to changes in seafloor type. Thus, we expect the present algorithms to give more accurate predictions of sediment physical properties, that is, to be better predictors of geoacoustic parameters. To improve acoustic prediction accuracy, it is recommended that a second set of regressions be performed using a cost function that combines both acoustic and geoacoustic error. These regressions would not supplant those provided here, as they would not provide the best estimates of physical properties. They would, rather, provide estimates of *effective* physical parameters, adjusted to correct deficiencies in the acoustic models.

Of significant importance to making acoustic predictions in the marine environment is the effect of hydrodynamic and biological processes on sediment properties. A major effect of sediment transport processes is sorting of grains, and hence the rationale behind incorporating this sediment parameter as an input for predicting geoacoustic properties. The sorting parameter, or graphic standard deviation (Folk, 1965), is a standard calculation found in any sediment grain size analysis. The chief effect of sorting appears to be on sediment sound speed. Low sorting values (well sorted) is indicative of faster sediment sound speeds. Percentages of grain size classes (gravel, sand, silt, and clay) have minor effects compared to the mean grain diameter (M_z). In the case of predicting the roughness power spectral exponent from grain size parameters, constituent proportions of sand, silt, and clay provide nearly equal effects on the value of the exponent (steepness), but only about half the variability in the exponent is explained by these constituents of the sediment.

It is important to note that there are no direct and accurate geoacoustic data to estimate one of the model parameters: σ_2 , the sediment volume scattering parameter. Clearly, more experimental work is needed to address the use of this parameter to predict high-frequency bottom backscatter.

Acknowledgments

This work was sponsored by SPAWAR, Program Element 63207N, Project Number X2342, Kim Koehler, program manager. This work was made possible with the help of Edward Chaika, CNMOC, Stennis Space Center, MS.

References

- Anonymous. 1994. "APL-UW High-Frequency Ocean Environmental Acoustic Models Handbook," APL-UW TR9407.
- Briggs, K.B., P. Fleischer, R.I. Ray, W.B. Sawyer, D.K. Young, M.D. Richardson and S. Stanic. 1986. "Environmental support for a high-frequency acoustic bottom backscatter experiment

- off Charleston, South Carolina, 17-28 June 1983,” Naval Research Laboratory, Stennis Space Center, MS. NORDA Report 130, 90p.
- Briggs, K.B. 1989. Microtopographical roughness of shallow-water continental shelves. *IEEE J. Ocean. Engin.*, 14: 360-367.
- Briggs, K.B., P. Fleischer, D.N. Lambert, R.I. Ray, and W.B. Sawyer. 1989. “Environmental support for high-frequency acoustic experiments conducted aboard the USNS BARTLETT, 2 August-3 September 1985,” Naval Research Laboratory, Stennis Space Center, MS. NORDA Tech. Note 458, 243p.
- Folk, R.L. 1965. *Petrology of Sedimentary Rocks*. Hemphill’s, Austin, Texas.
- Hamilton, E.L. and R.T. Bachman. 1982. Sound velocity and related properties of marine sediments,” *J. Acoust. Soc. Am.*, 72: 1891-1904.
- Jackson, D.R. and K.B. Briggs. 1992. High-frequency bottom backscattering: roughness vs. sediment volume scattering. *J. Acoust. Soc. Am.*, 92: 962-977.
- Jackson, D.R., K.B. Briggs, K.L. Williams, and M.D. Richardson. 1996. Tests of models for high-frequency seafloor backscatter. *IEEE J. Ocean. Engin.*, 21: 458-470.
- Richardson, M.D., D.K. Young, and R.I. Ray. 1983. “Environmental Support for High Frequency Acoustic Measurements at NOSC Oceanographic Tower, 26 April-7 May 1982; Part I: Sediment Geoacoustic Properties,” Naval Research Laboratory, Stennis Space Center, MS, NORDA Tech. Note 219, 68p.
- Richardson, M.D., J.H. Tietjen, and R.I. Ray. 1983. “Environmental Support for Project WEAP East of Montauk Point, New York 7-28 May 1982,” Naval Research Laboratory, Stennis Space Center, MS, NORDA Rep. 40, 52p.
- Richardson, M.D., K.B. Briggs, L.D. Bibee, P.A. Jumars, W.B. Sawyer, et al. 2001. Overview of SAX99: Environmental considerations. *IEEE J. Oceanic Engin.*, 26: 26-53.
- Richardson, M.D., K.B. Briggs, S.J. Bentley, D.J. Walter and T.H. Orsi. 2002. Biological and hydrodynamic effects on physical and acoustic properties of sediments off the Eel River, California. *Mar. Geol.*, 182: 121-139.
- Self, R.F.L., P. A’Hearn, P.A. Jumars, D.R. Jackson, M.D. Richardson, and K.B. Briggs. 2001. Effects of macrofauna on acoustic backscatter from the seabed: Field manipulations in West Sound, Orcas Island, WA, USA. *J. Mar. Res.*, 59: 991-1020.
- Stanic, S., K.B. Briggs, P. Fleischer, R.I. Ray, and W.B. Sawyer. 1988. Shallow-water high-frequency bottom scattering off Panama City, Florida. *J. Acoust. Soc. Am.*, 83: 2134-2144.
- Stanic, S., K.B. Briggs, P. Fleischer, W.B. Sawyer, and R.I. Ray. 1989. High-frequency acoustic backscattering from a coarse shell ocean bottom. *J. Acoust. Soc. Am.*, 85: 125-136.

Table 1. Geoacoustic properties used to predict high-frequency backscatter from the sea floor. Units are expressed as m/s (Vp), m²/s² (σ^2_V), dB/m (α), phi (M_z), percent (β), g/cm³ (ρ), cm (l_c), dB/m/kHz (k), and cm³ (w₁).

Site	Vp	VpR	σ^2_V	α	M _z	β	ρ	ρ Ratio	σ^2_{rho}	l _c	k	Type	γ_1	w ₁
KB/lyn	1700.2	1.112	697.03	567.7	0.90	39.50	2.031	1.985	0.00124	5.02	1.419	hash	1.47	0.00534
Misby/crse	1755.5	1.148	601.81	140.0	0.95	32.55	2.120	2.073	8.50E-05	1.44	0.350	coarse sand	2.46	0.00570
PC93	1698.6	1.111	329.06	391.2	0.98	40.27	2.021	1.975	0.00101	2.45	0.874	coarse sand	2.12	0.00198
SAX99	1765.8	1.155	89.15	173.5	1.27	36.60	2.074	2.027	0.00025	3.51	0.434	rip.med sand	2.54	0.00077
KB/bar	1750.2	1.144	230.7	209.3	1.33	36.76	2.055	2.009	0.00052	6.05	0.523	med sand	1.90/2.06	0.00094
Charl/crse	1716.8	1.123	206.24	295.3	1.44	39.40	2.009	1.959	0.00044	4.29	0.738	med sand	2.05	0.00008
Charl/fine	1721.8	1.126	206.19	218.9	1.97	39.80	2.004	1.954	0.00053	3.68	0.547	fine sand	2.29/1.33	0.00008/0.00054
JDF2	1762.9	1.153	328.87	168	2.03	38.54	2.048	2.004	0.00078	5.73	0.420	med sand		
MonPt	1733.6	1.134	149.62	89.1	2.04	36.68	2.054	2.003	0.00005	3.11	0.223	fine sand	2.72	0.00003
JDF5	1704.1	1.107	354.72	206.7	2.31	44.81	1.956	1.912	0.00488	2.38	0.517	fine sand/s-s-c		
PC84	1732.4	1.133	100.17	233.8	2.61	39.45	2.008	1.963	0.00013	5.03	0.584	fine sand	1.89	0.00233
JDF6	1669.3	1.086	1921.19	303.2	2.94	46.90	1.932	1.890	0.01037	2.65	0.758	fine sand/s-s-c		
Quinault	1700.4	1.112	320.08	171.4	2.94	41.12	1.980	1.937	0.00066	3.53	0.429	fine sand	2.67/2.92	0.00033/0.00028
Tirr	1681.6	1.095	18.43	123.4	3.72	45.76	1.906	1.863	9.60E-05	5.68	0.309	v.fine sand	3.01	2.55E-04
Misby/fine	1674.1	1.095	424.32	189.3	3.77	49.14	1.850	1.808	0.00242	2.38	0.473	fine sand	2.17	0.00123
JDF1	1615.3	1.056	58.86	236.3	4.37	54.53	1.813	1.774	0.00076	2.06	0.591	silty fine sand		
Arafura	1510.4	0.988	29.14	336.4	5.24	70.48	1.510	1.478	0.00281	5.25	0.841	clayey sand	2.18	0.00069
RussRiver	1543.3	1.009	35.33	223.4	6.35	63.40	1.610	1.580	0.00025	3.31	0.559	clayey sand	2.50/2.70	0.00013/0.00006
KW	1553.2	1.017	48.71	333.3	6.62	58.30	1.760	1.720	0.00068	2.19	0.833	carb. s-s-clay	2.29	0.00209
JDF4	1519.2	0.993	10.50	196.5	6.93	73.19	1.489	1.457	0.00050	4.24	0.491	glacial till		
ER	1555.6	1.017	324.72	210.1	7.17	55.40	1.788	1.748	0.00211	2.53	0.525	clayey-silt	3.28	5.60E-05
Orcas	1510.6	0.988	6.34	173.2	8.08	74.10	1.420	1.388	0.00032	3.33	0.433	clayey sand	3.23	5.20E-05
JDF7	1506.0	0.985	1.073	110.6	8.50	82.13	1.369	1.340	0.00010	2.97	0.277	silty clay		

Table 2. Surficial (0-2 cm) values for geoaoustic input parameters. Units are the same as in Table 1.

0-2cmvalues	VpR	α	M_z	β	ρ	ρ Ratio	k
KB/lyn	1.087	645.4	0.51	41.75	2.001	1.956	1.614
Misby/crse	1.128	117.6	0.91	32.27	2.125	2.077	0.294
PC93	1.097	417.5	0.68	42.67	1.993	1.948	1.044
SAX99	1.145	141.0	1.28	36.6	2.073	2.026	0.352
KB/bar	1.136	190.0	1.33	37.59	2.043	1.997	0.475
Charl/crse	1.113	309.3	1.33	39.93	2.002	1.957	0.773
JDF6	1.083	357.2	1.83	49.33	1.88	1.838	0.893
Charl/fine	1.125	154.2	1.94	39.73	2.005	1.960	0.386
JDF2	1.147	148.1	2.04	37.49	2.062	2.016	0.370
MonPt	1.12	99.6	2.09	37.5	2.041	1.995	0.249
JDF5	1.092	200.1	2.23	48.13	1.900	1.857	0.500
PC84	1.115	236.3	2.63	41.59	1.973	1.929	0.591
Quinault	1.113	118.8	2.95	40.3	2.001	1.956	0.297
Tirr	1.096	124.6	3.57	44.97	1.919	1.876	0.312
Misby/fine	1.085	178.2	3.85	49.66	1.842	1.801	0.446
JDF1	1.042	213.2	3.85	59.82	1.711	1.673	0.533
Arafura	0.988	204.3	5.65	78.7	1.376	1.345	0.511
RussRiver	1.002	147.1	6.39	72.83	1.488	1.455	0.368
JDF4	0.995	131.0	6.86	78.93	1.379	1.348	0.327
KW	1.003	217.7	7.00	70.91	1.533	1.499	0.544
ER	1.016	268.7	7.39	61.9	1.674	1.636	0.672
Orcas	0.992	113.8	8.34	83.18	1.279	1.250	0.285
JDF7	0.988	70.1	8.79	88.03	1.23	1.202	0.175

Table 3. Average values of geoacoustic parameters for predicting acoustic backscattering. Location data are given in the cited publications.

Site	VpR	k	ρ	gravel	sand	silt	clay	M _z	sorting	sigma-2	γ_1	w ₂	Cit.
KB/lyn	1.105	1.496	2.035	19.38	77.61	1.57	1.43	0.90	1.70	0.000061	1.47	0.00522	[1]
PC93	1.105	1.001	2.012	3.60	92.96	1.40	2.04	0.90	1.01	0.000112	2.12	0.00849	[2]
Misby/crse	1.151	0.337	2.120	0.72	96.57	2.00	0.71	0.96	0.91	0.000054	2.46	0.00473	[3]
SAX99	1.155	0.430	2.076	0.69	98.05	0.42	0.84	1.26	0.64	0.000035	2.54	0.00755	[4]
KB/bar	1.144	0.550	2.056	2.16	96.39	0.50	0.95	1.32	0.87	0.000053	1.90	0.00238	[5]
Charl/crse	1.121	0.768	2.009	5.39	92.84	0.71	1.06	1.51	1.10	0.000041	2.05	0.00028	[6]
Charl/fine	1.123	0.682	2.012	3.73	94.39	0.92	0.99	1.85	0.93	0.000066	2.29	0.00046	[6]
JDF2	1.154	0.421	2.052	0.03	94.67	2.52	2.78	2.03	0.85	0.006000			Table 3A
MonPt	1.137	0.237	2.052	0.02	98.04	0.99	0.95	2.04	0.67	0.000046	2.72	0.00043	[7]
JDF5	1.115	0.457	1.990	0.00	89.07	5.23	5.70	2.31	1.38	0.003000			Table 3A
PC84	1.132	0.585	2.010	1.92	91.12	4.22	2.74	2.61	1.11	0.000018	1.89	0.00590	[8]
JDF6	1.081	0.780	1.880	1.43	74.83	13.15	10.59	2.88	2.58	0.000712			Table 3A
Quinault	1.112	0.425	1.983	0.30	92.61	4.16	2.94	2.93	0.94	0.000112	2.67	0.00422	[9]
Tirr	1.097	0.308	1.909	0.00	82.18	11.00	6.82	3.72	1.41	0.000014	3.01	0.00654	Table 3A
Misby/fine	1.092	0.453	1.850	0.14	85.11	13.03	1.73	3.72	1.37	0.000301	2.17	0.00555	[3]
JDF1	1.056	0.608	1.817	0.11	57.06	32.84	9.99	4.37	1.87	0.002000			Table 3A
Arafura	0.988	0.877	1.515	11.12	44.51	10.49	33.88	5.26	5.53	0.005000	2.18	0.00318	[9]
RussRiver	1.009	0.543	1.609	0.00	16.40	61.91	21.69	6.37	2.96	0.002000	2.50	0.00100	[9]
KW	1.017	0.826	1.767	0.64	28.64	36.10	34.62	6.62	3.75	0.000112	2.29	0.01220	[2]
JDF4	0.994	0.489	1.483	0.00	12.58	57.79	29.63	6.92	2.82	0.002000			Table 3A
ER	1.021	0.514	1.802	0.00	8.98	56.55	34.47	7.23	2.77	0.001281	3.28	0.00248	[11]
Orcas	0.988	0.437	1.428	0.06	1.21	56.62	42.11	8.10	2.74	0.000291	3.23	0.00208	[12]
JDF7	0.984	0.275	1.333	0.02	0.64	47.83	51.51	8.51	2.49	0.002000			Table 3A

[1] Stanic et al., 1989, [2] Jackson et al., 1996, [3] Richardson et al., 1983, [4] Richardson et al., 2001, [5] Briggs et al., 1989, [6] Briggs et al., 1986, [7] Richardson et al., 1983, [8] Stanic et al., 1988, [9] Jackson and Briggs, 1992, [10] Richardson et al., 2002, [11] Self et al., 2002. **Table 3A:** Previously unpublished data.

Table 3A. Location information for Strait of Juan de Fuca and Tirrenia geoacoustic data. Water depth is in meters.

Site	Latitude	Longitude	Water Depth
JDF1	48°18'N	124°54'W	165
JDF2	48°13'N	125°09'W	117
JDF4	48°07'N	125°16'W	280
JDF5	48°23'N	125°36'W	145
JDF6	48°24'N	125°33'W	133
JDF7	48°26'N	125°25'W	156
Tirr	43°38'N	10°17'W	8

Table 4. Fits between model and data using four sources of parameters for the 18 sites available for model-data comparisons. Key: B = best fit; b = acceptable fit; blank = poor fit.

source	KB/lyn	PC93	SAX99	JDF6	JDF2	MonPt	JDF5	PC84	Quinault	Tirr	JDF1	Arafura	RussRiver	KW	JDF4	ER	Orcas	JDF7
Sing. Regr.	b								b		b	b		B			B	
Mult. Regr.	b				b								b	B	b		B	
Avg. 0-2cm	b	B	B	B			b	b	b					b		b		
TR9407	b	B		B	b		B	b	B		B			B			B	

Table 5. Errors (in dB) for the model-data fit for single regression algorithm under “SR” column, for the multiple regression algorithm under the “MR” column, for the surficial geoaoustic data under column “SURF” and for using APL-UW’s TR9407 grain size description under column “9407”.

Site	Error (dB)			
	SR	MR	SURF	9407
KB/lyn	2.998	2.868	3.989	3.497
PC93	4.131	8.571	1.912	1.550
SAX99	6.345	11.34	1.425	5.308
JDF6	13.19	9.061	1.625	1.874
JDF2	11.70	2.592	4.725	3.267
MonPt	18.66	4.830	18.09	11.47
JDF5	7.718	4.782	3.202	1.690
PC84	5.471	4.406	2.818	3.894
Quinault	2.955	5.598	3.674	1.424
Tirr	7.088	14.12	7.879	9.302
JDF1	2.547	6.680	9.956	1.930
Arafura	3.475	7.730	9.386	5.437
RussRiv	5.644	3.766	13.79	5.825
JDF4	5.009	2.230	14.27	4.785
KW	1.052	1.404	2.962	1.374
ER	8.643	5.793	3.469	9.508
Orcas	0.896	1.027	5.398	1.417
JDF7	4.231	4.216	17.62	5.215
Mean error	6.54	5.61	7.01	4.38

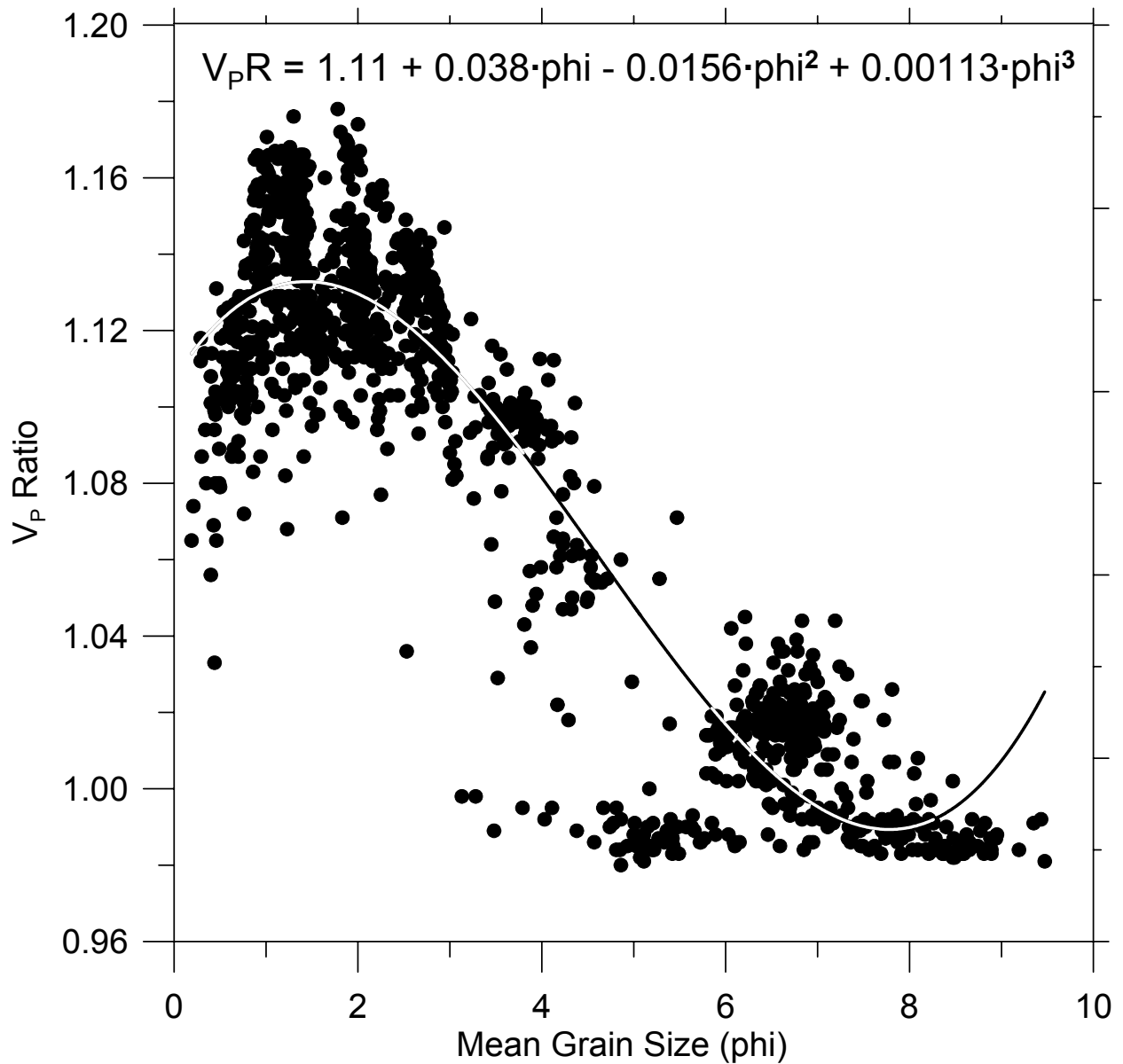


Figure 1. Scatter plot of sound speed ratio ($V_p R$) as a function of mean grain size (ϕ) using all data from all cores. Third-degree polynomial regression fit has an r^2 of 0.86.

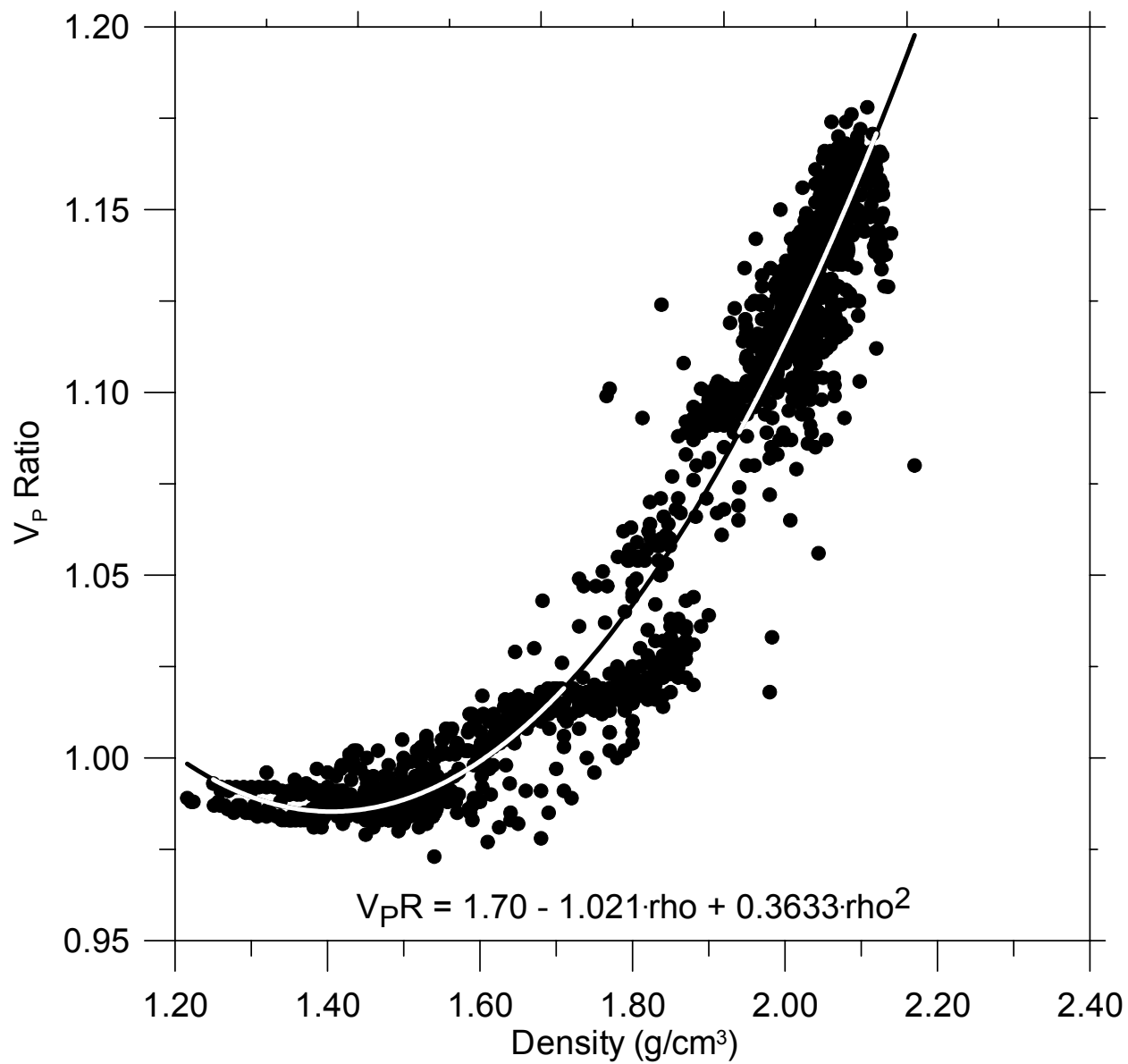


Figure 2. Scatter plot of sound speed ratio as a function of bulk density (ρ) using all data from all cores. Second-degree polynomial regression fit has an r^2 of 0.94.

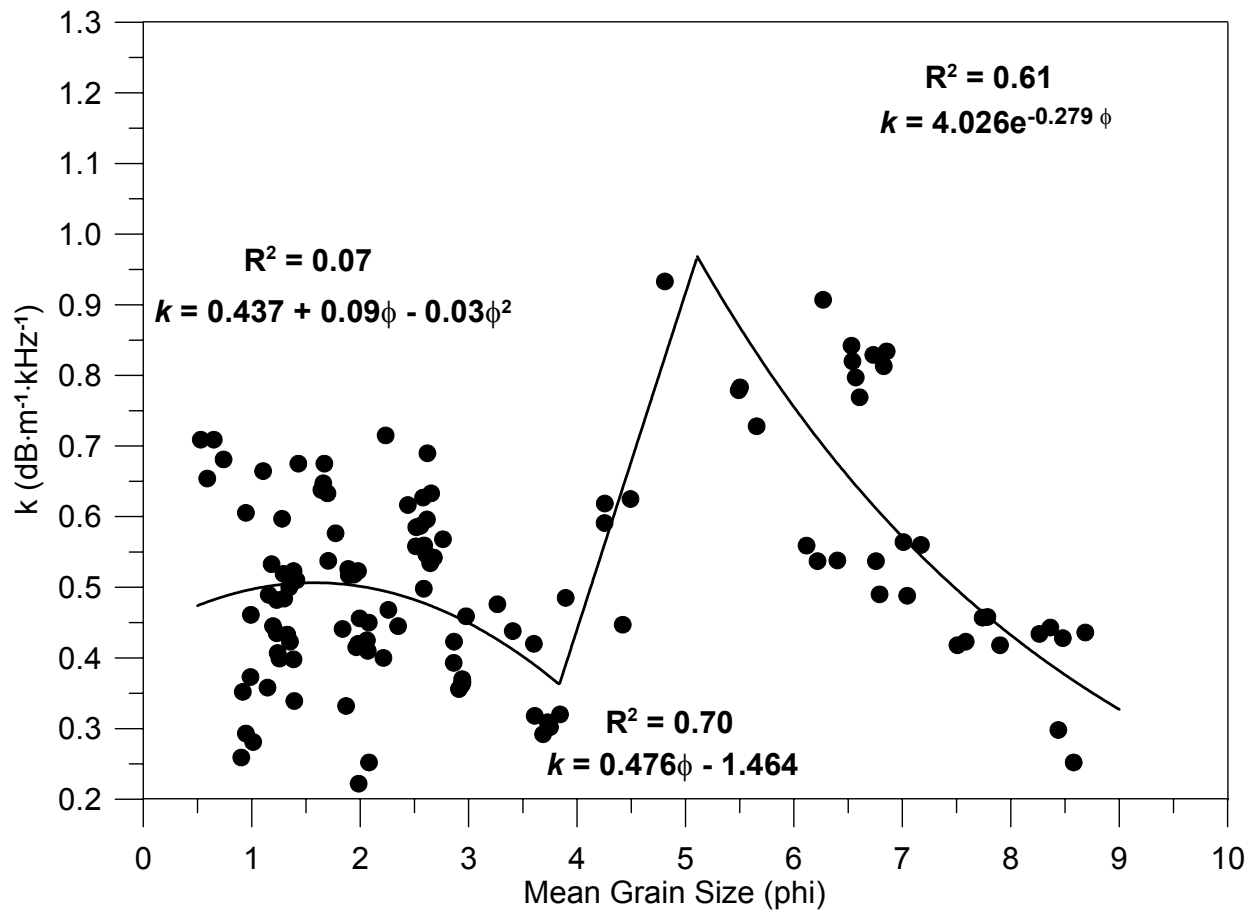


Figure 3. Piecewise regression fit of scatter plot of sound attenuation (k) as a function of mean grain size (ϕ) using only averaged core data.

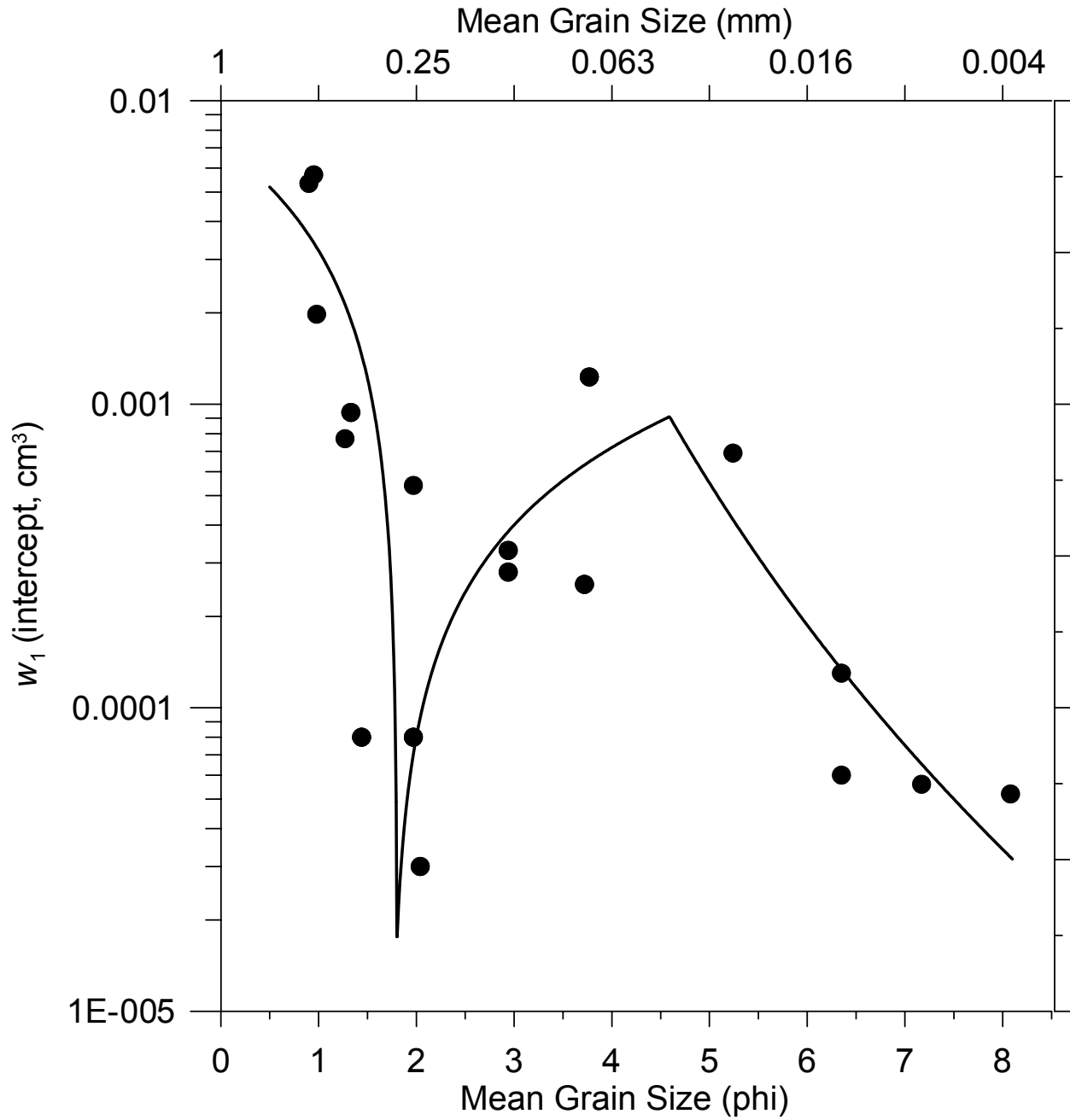


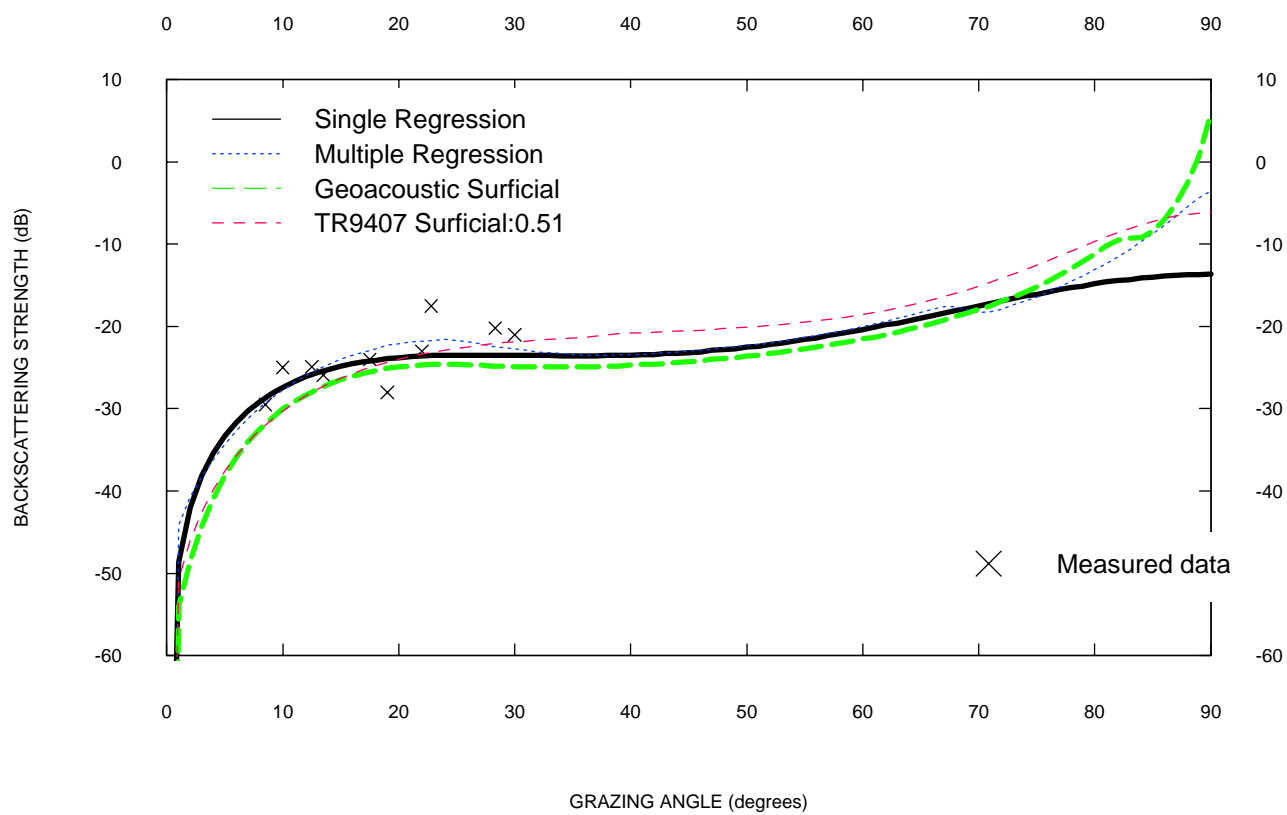
Figure 4. Piecewise regression fit of scatter plot of roughness power spectral intercept (w_1) as a function of mean grain size (ϕ) using only averaged data from each site.

Appendix 1

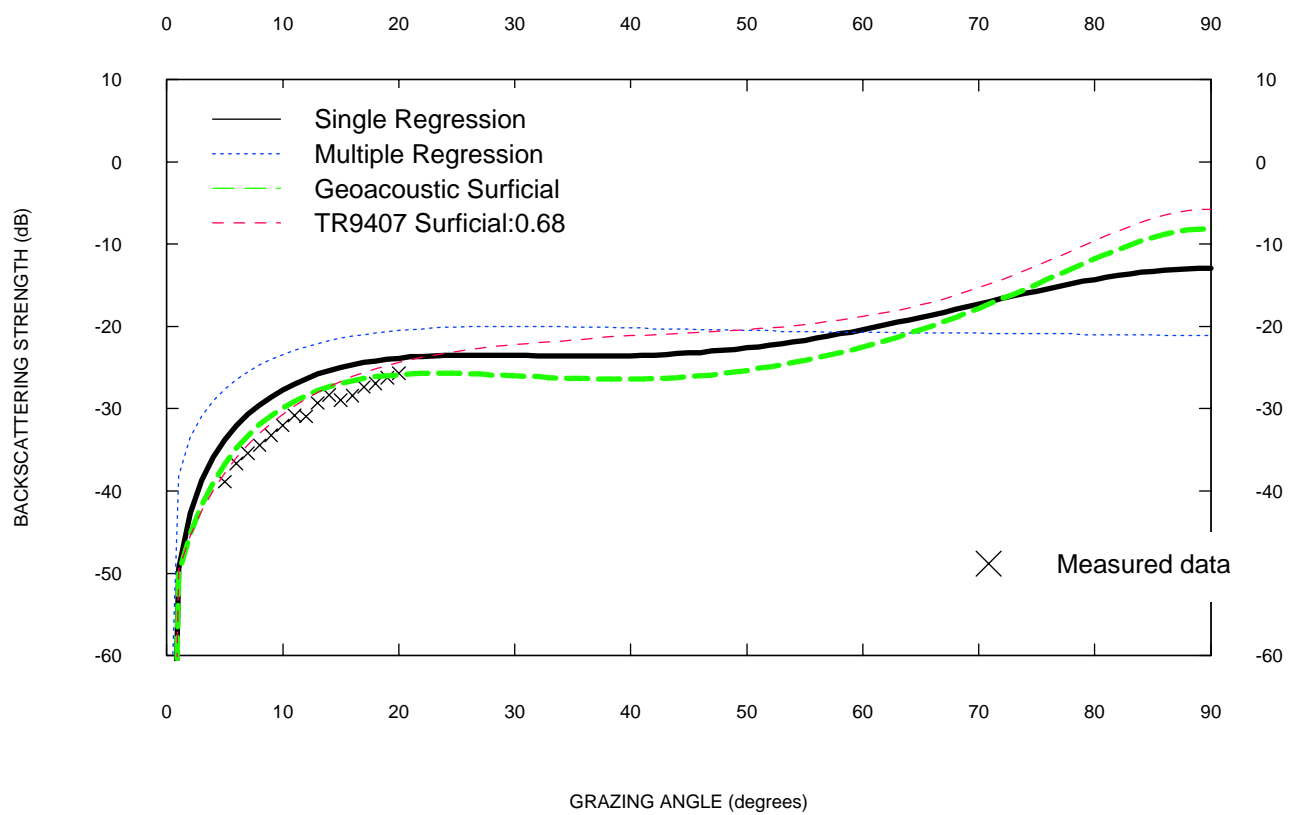
The following 18 plots of predicted backscattering strength as a function of grazing angle include measured backscattering data for comparison. Four predictions are made for each of the 18 sites, generated from input parameters derived from single regression (usually mean grain size), multiple regression (grain size parameters), surficial geoacoustic parameters, or the grain size algorithm contained in APL-TR-9407. The plots appear in the following order:

KB_lyn
PC93
SAX99
JDF6
JDF2
MonPt
JDF5
PC84
Quinault
Tirr
JDF1
Arafura
RussRiver
KW
JDF4
ER
Orcas
JDF7

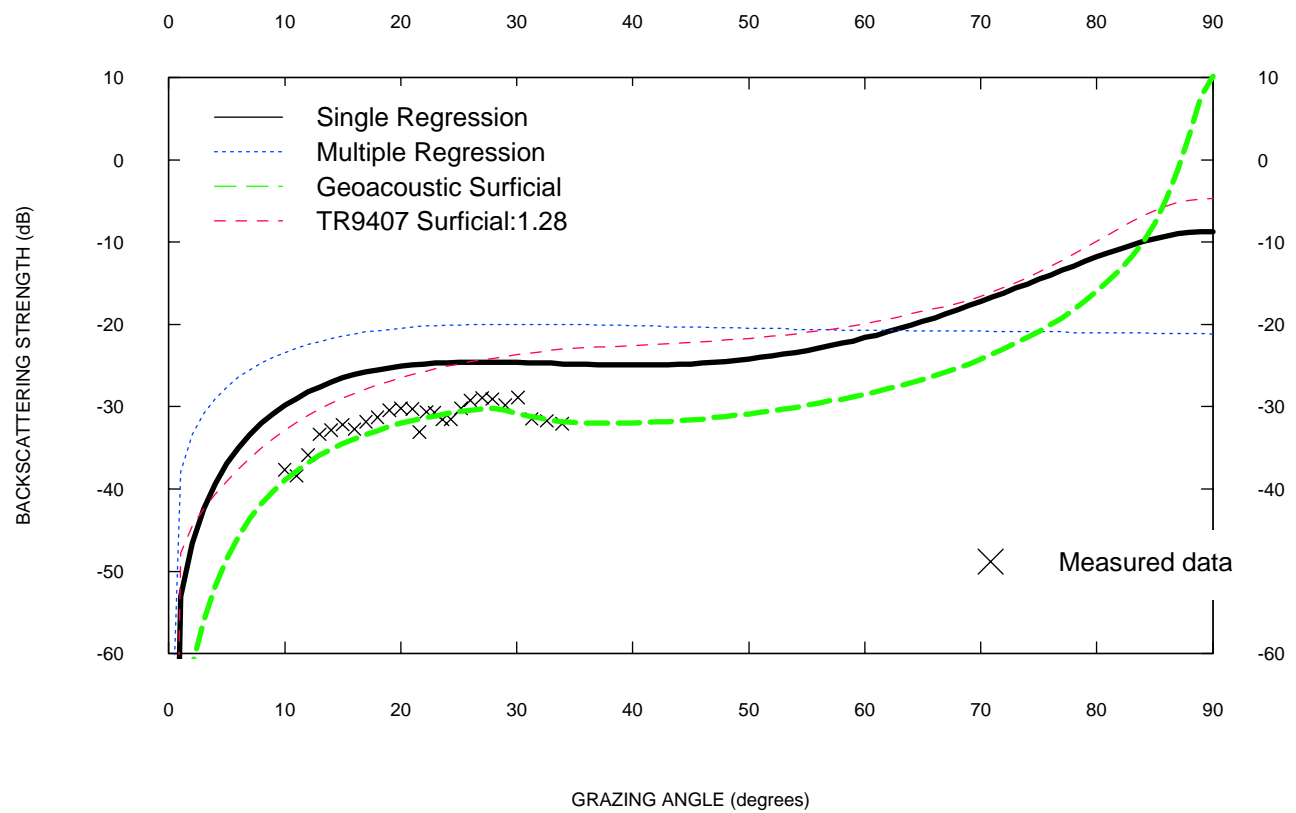
Kings_Bay_Lyn_ backscattering at 40 kHz



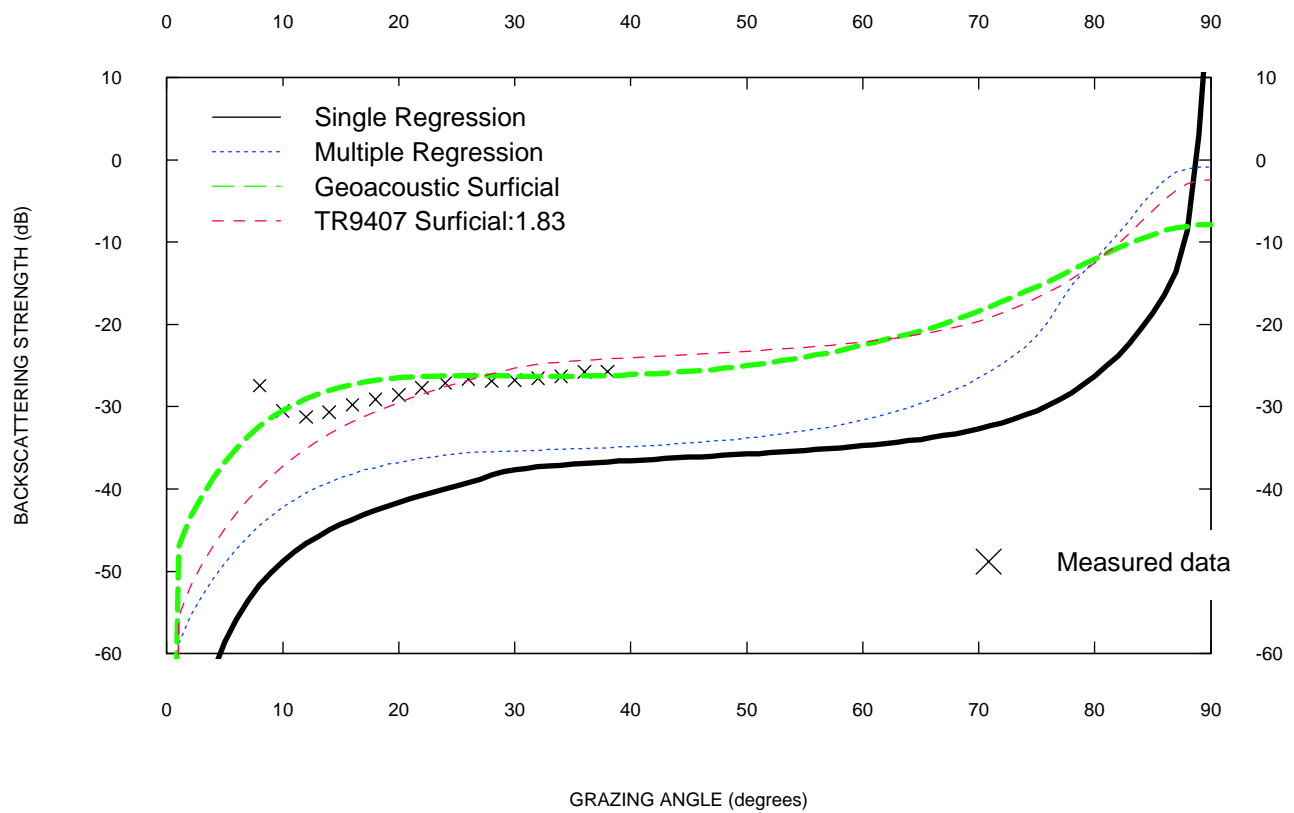
Panama_City_1993 backscattering at 40 kHz



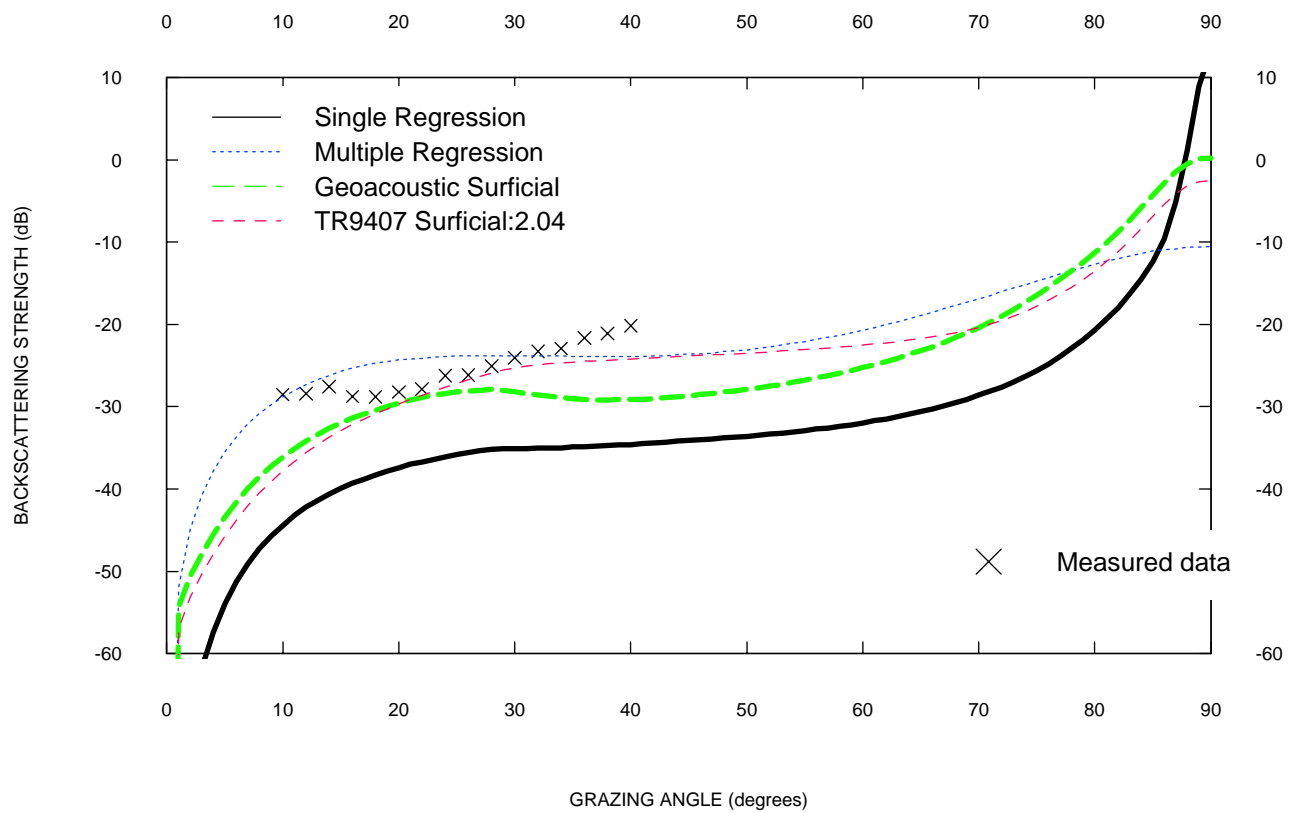
SAX_1999 backscattering at 40 kHz



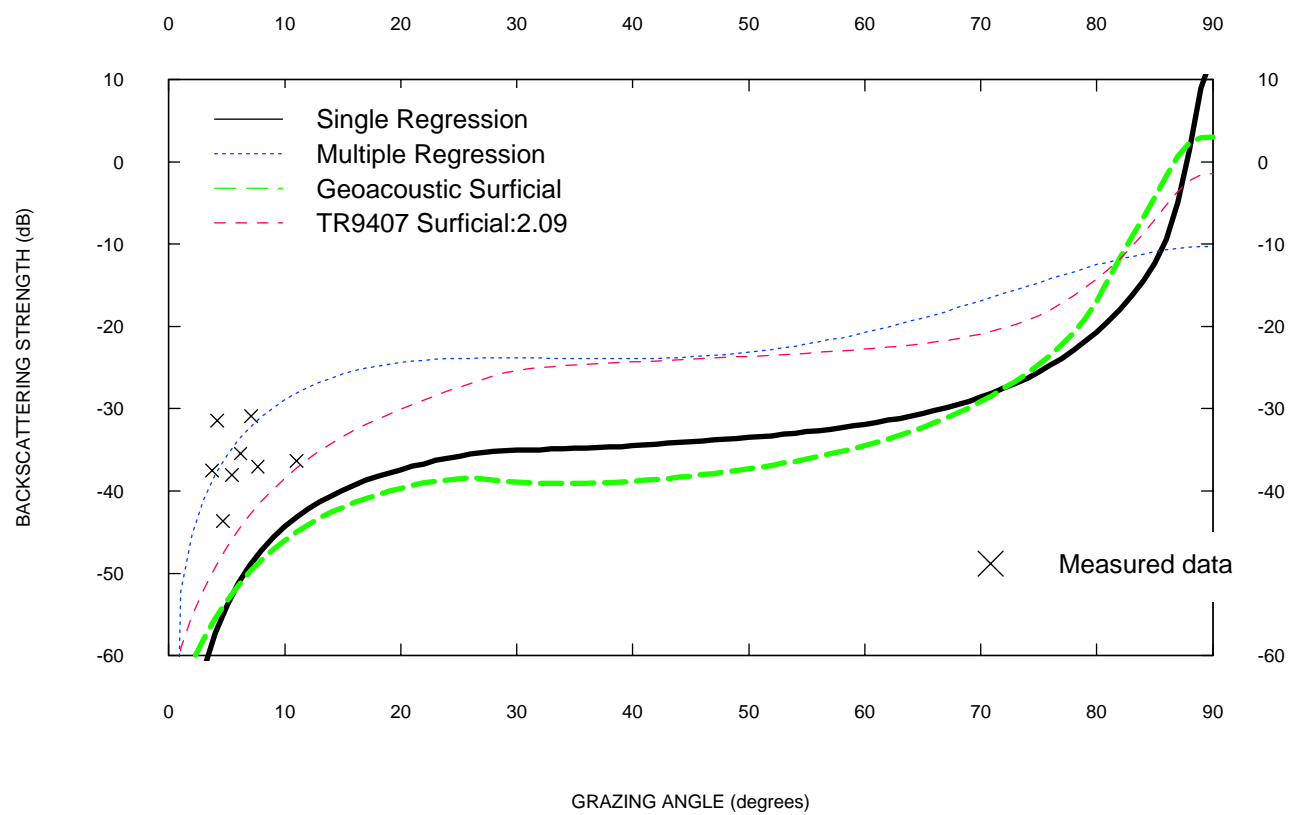
Juan_de_Fuca_Site6 backscattering at 25 kHz



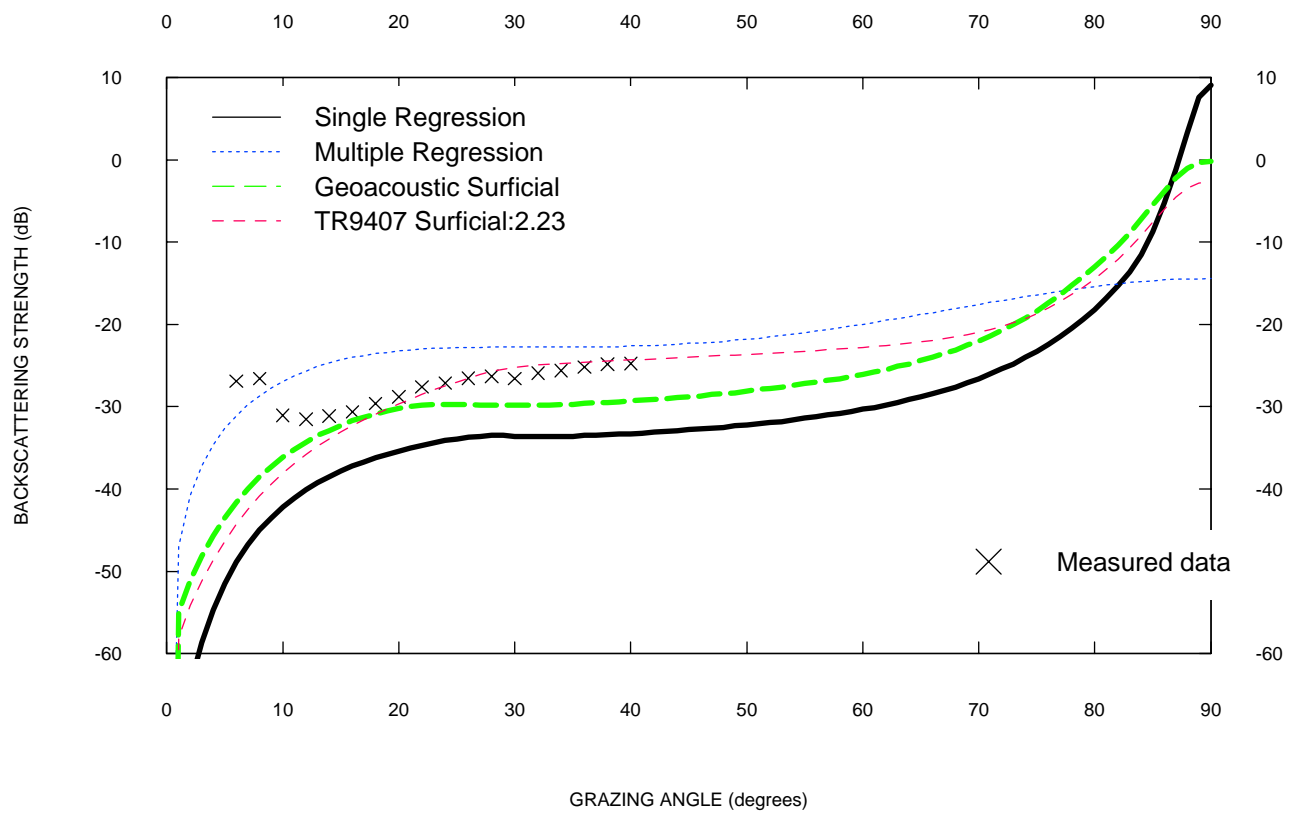
Juan_de_Fuca_Site2 backscattering at 25 kHz



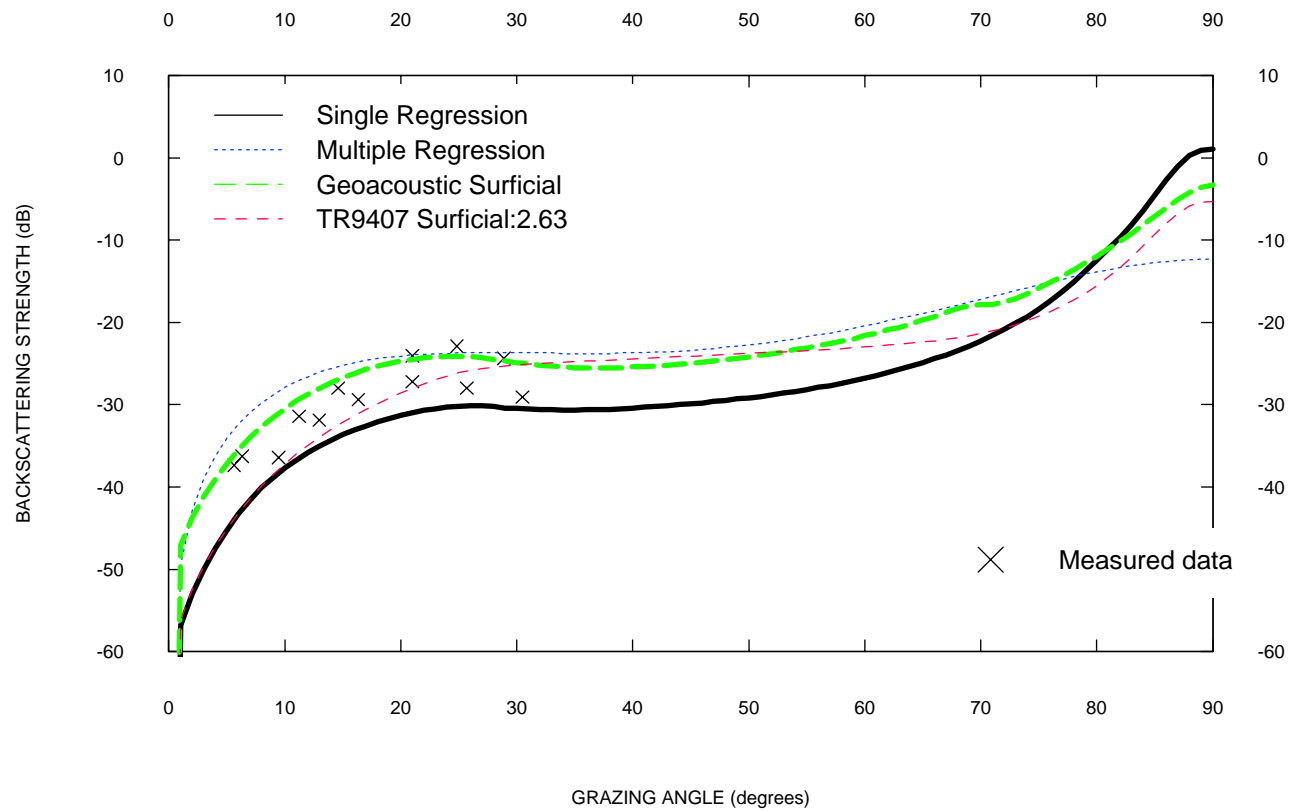
MonTauk_Point_1984 backscattering at 20 kHz



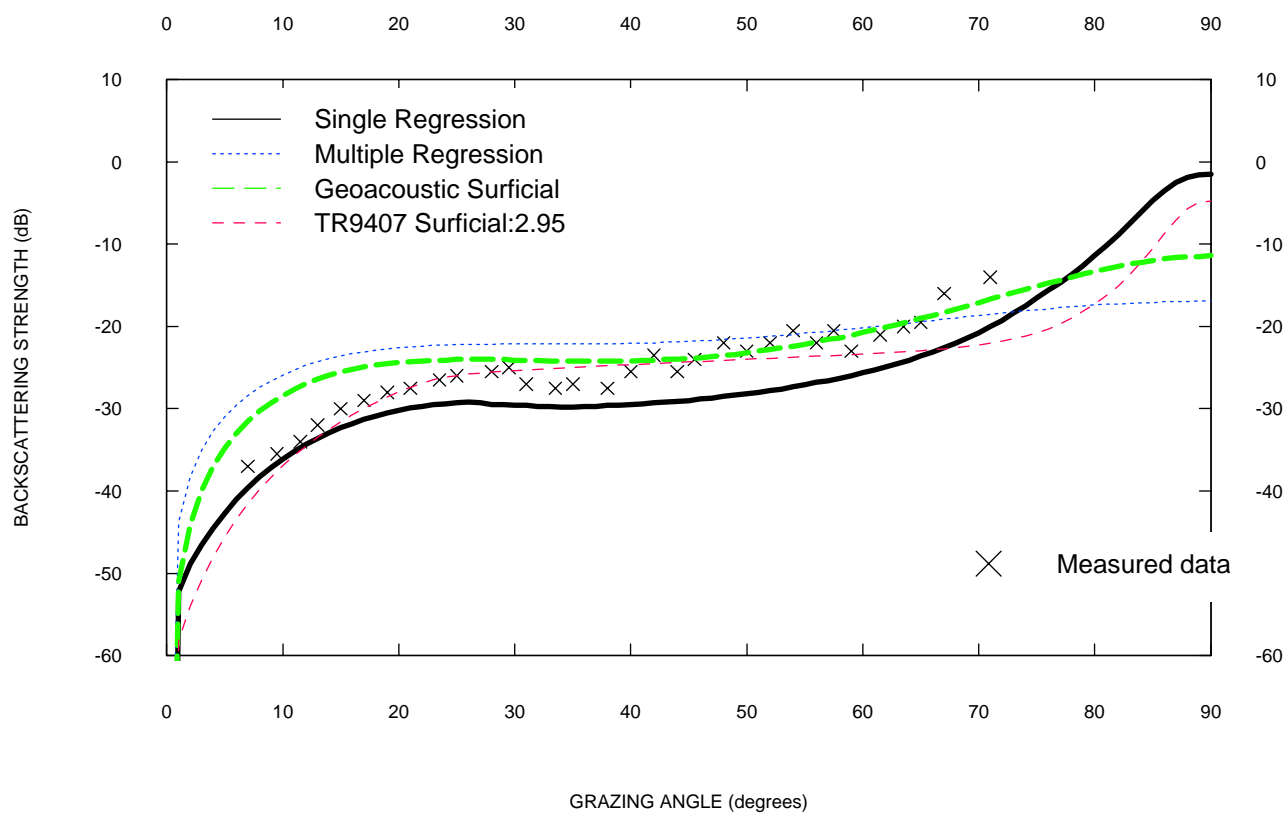
Juan_de_Fuca_Site5 backscattering at 25 kHz



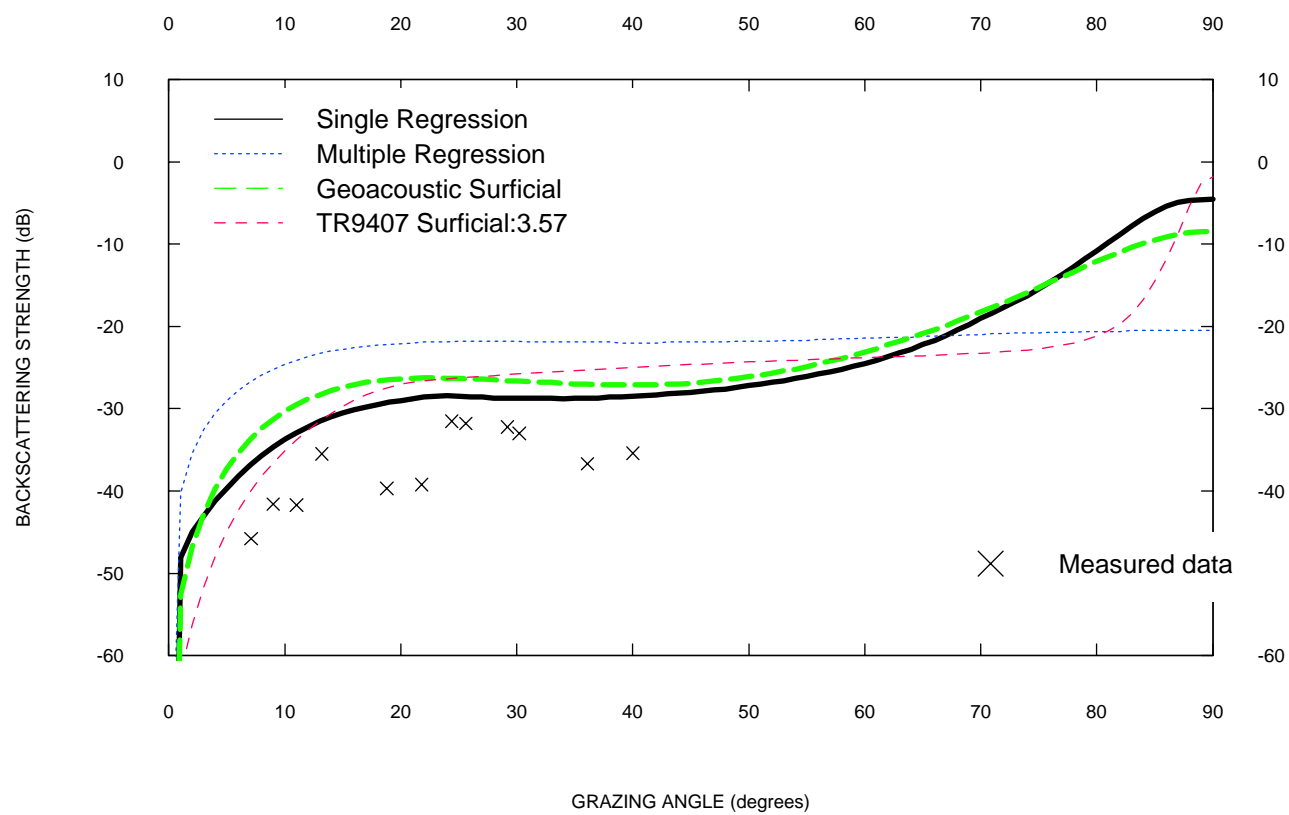
Panama_City_1984 backscattering at 40 kHz



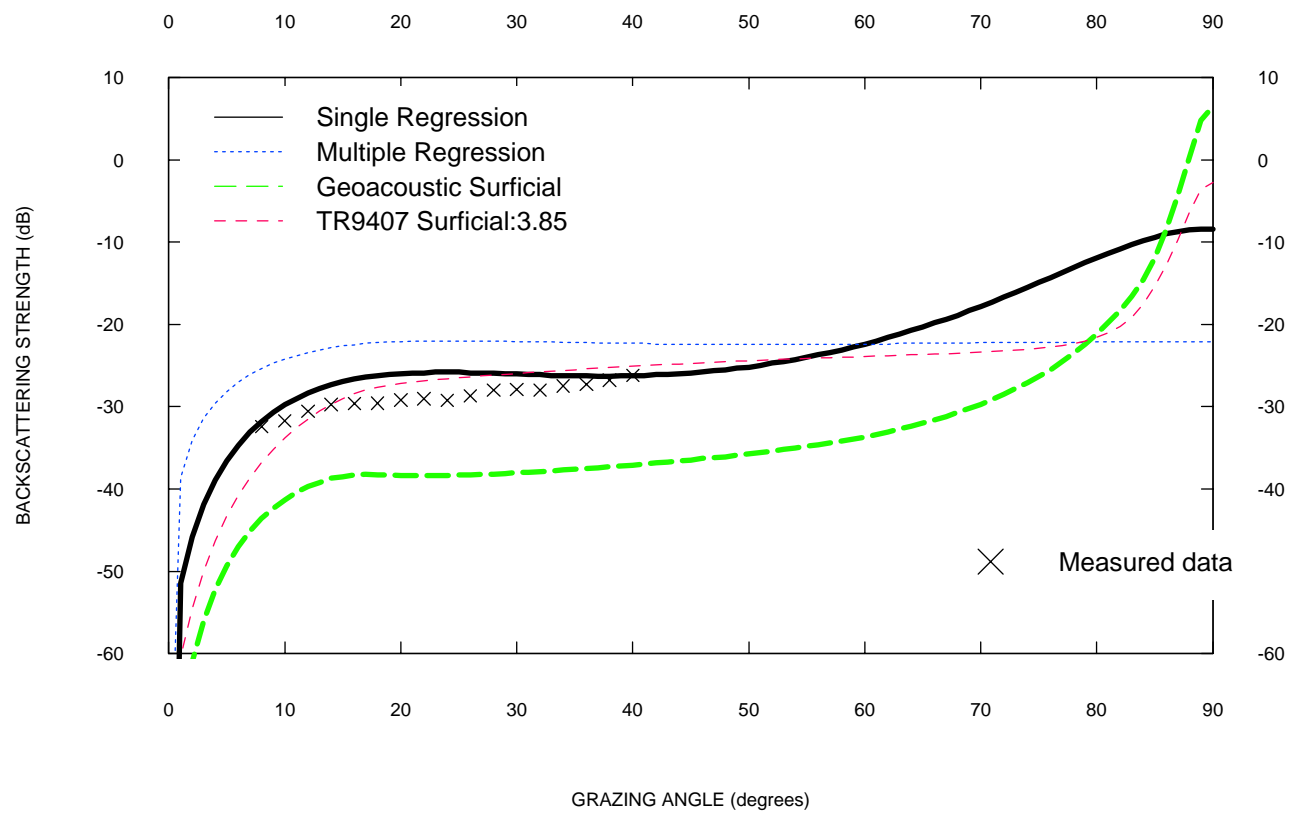
Quinault backscattering at 35 kHz



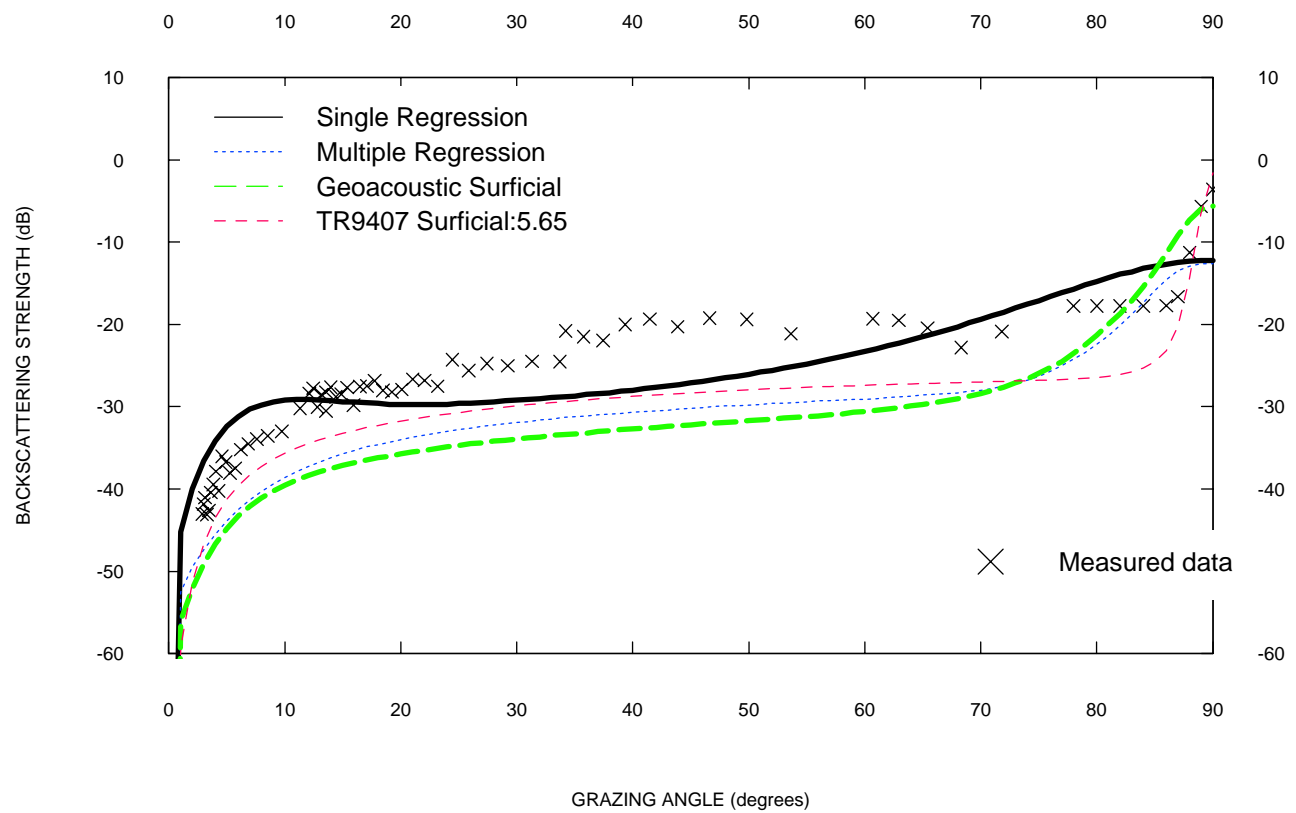
Tirrenia backscattering at 20 kHz



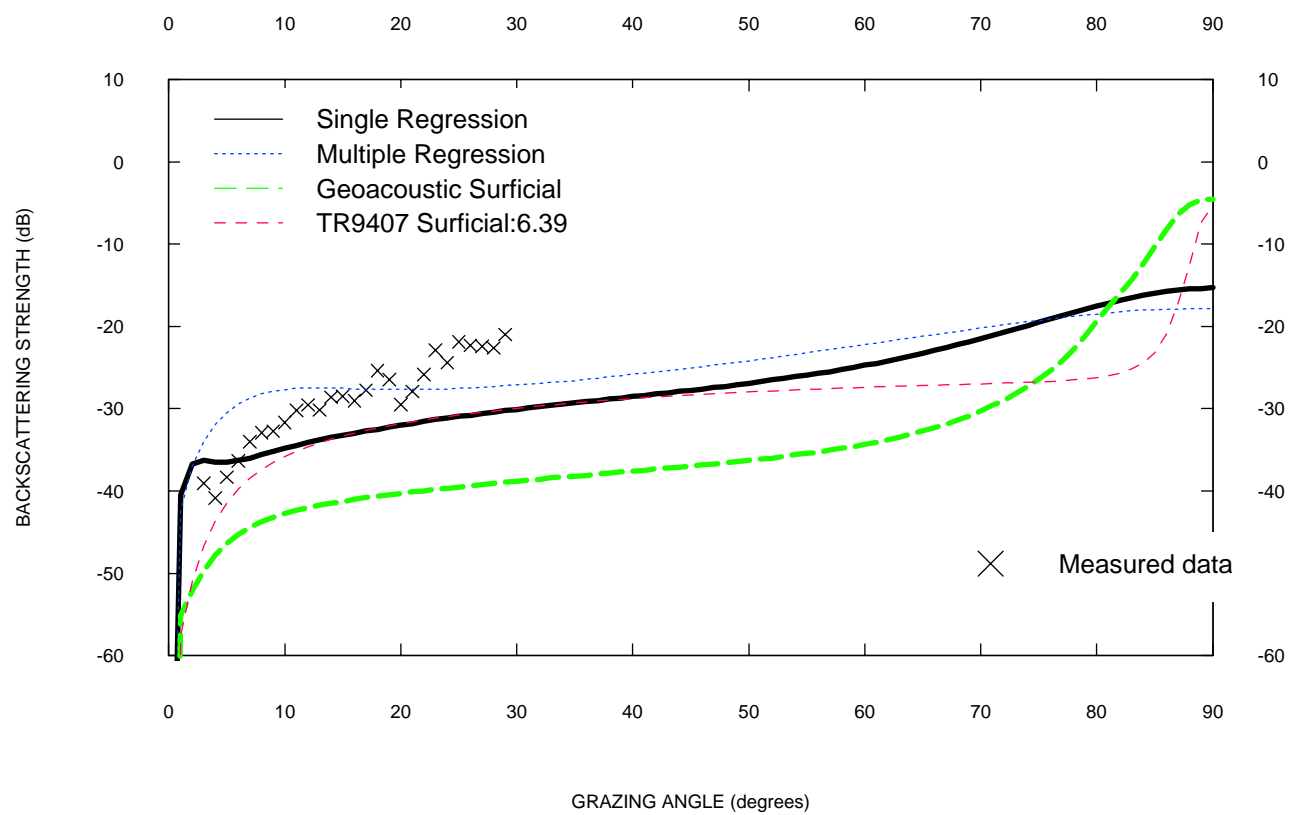
Juan_de_Fuca_Site1 backscattering at 25 kHz



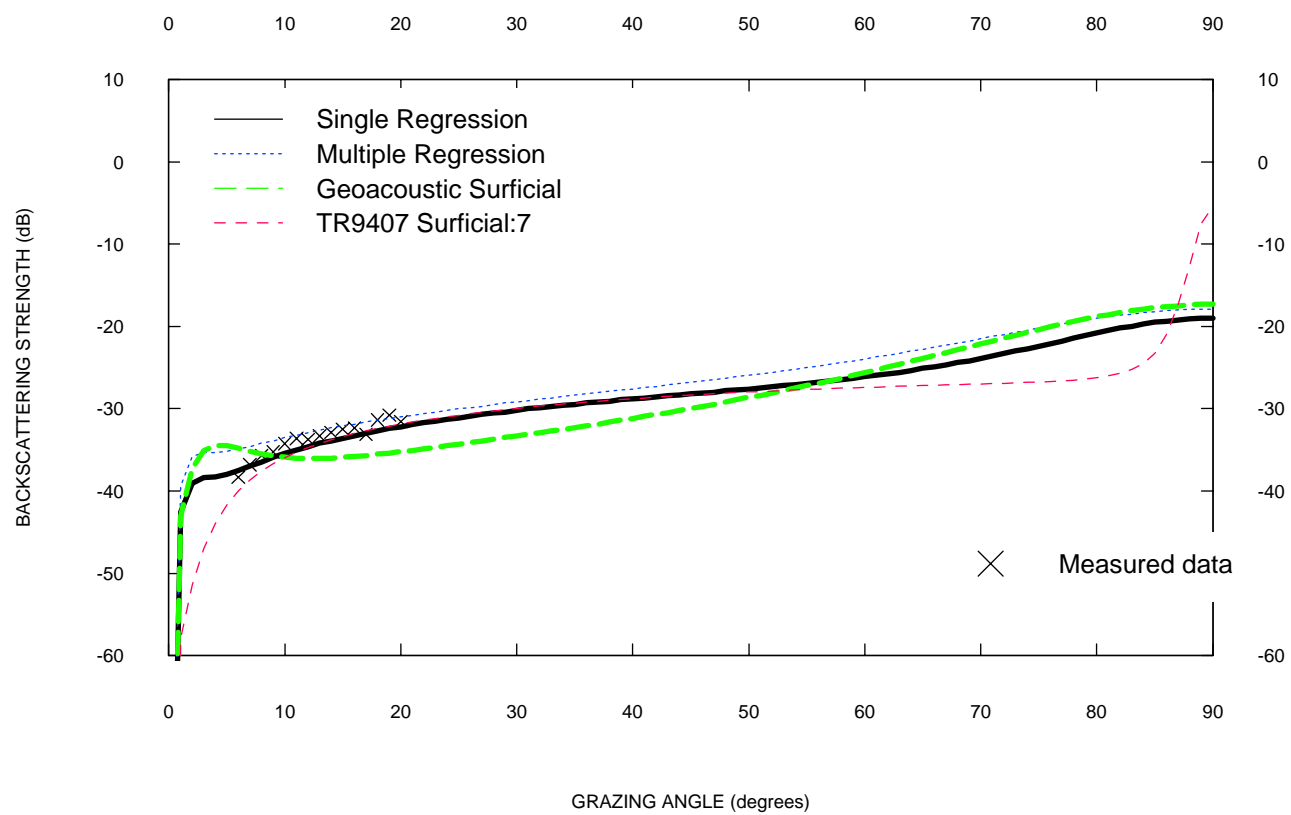
Arafura backscattering at 20 kHz



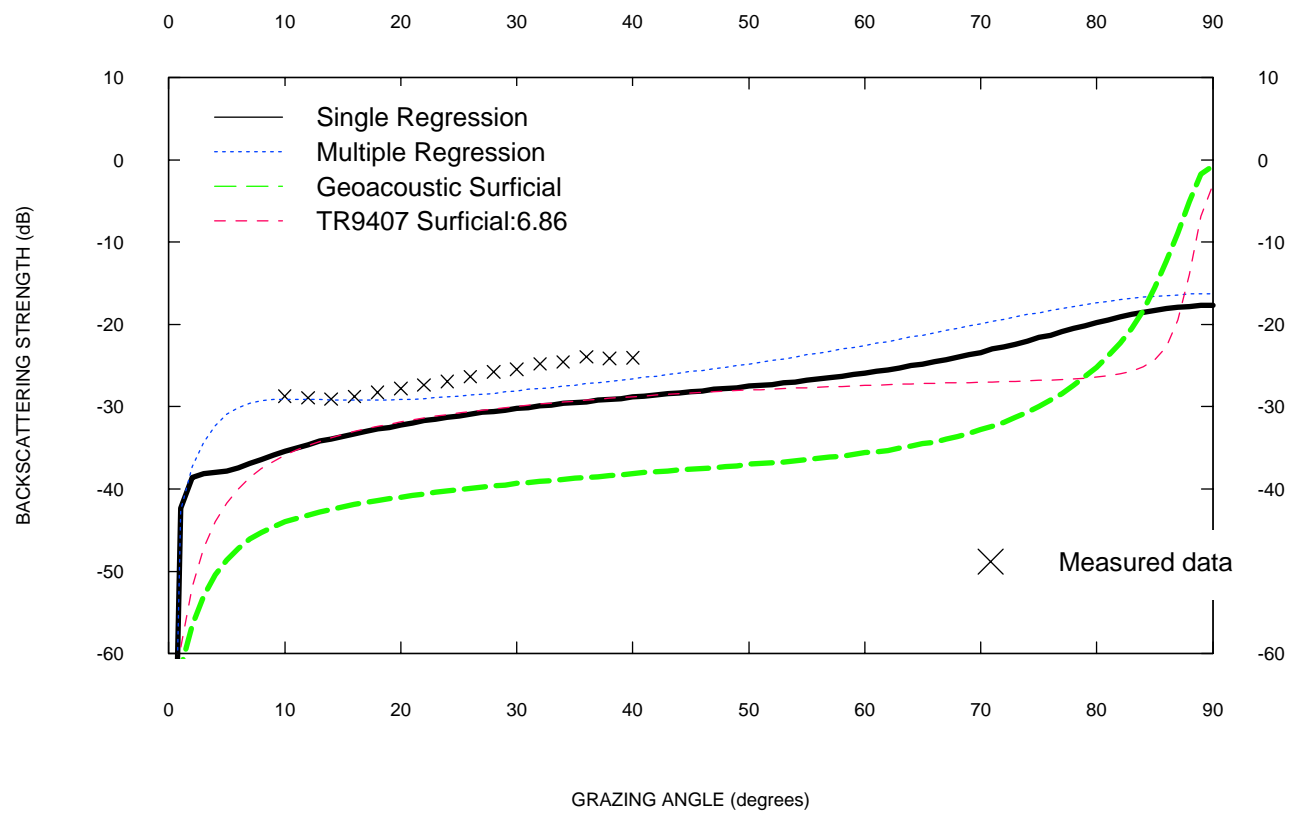
Russian_River backscattering at 40 kHz



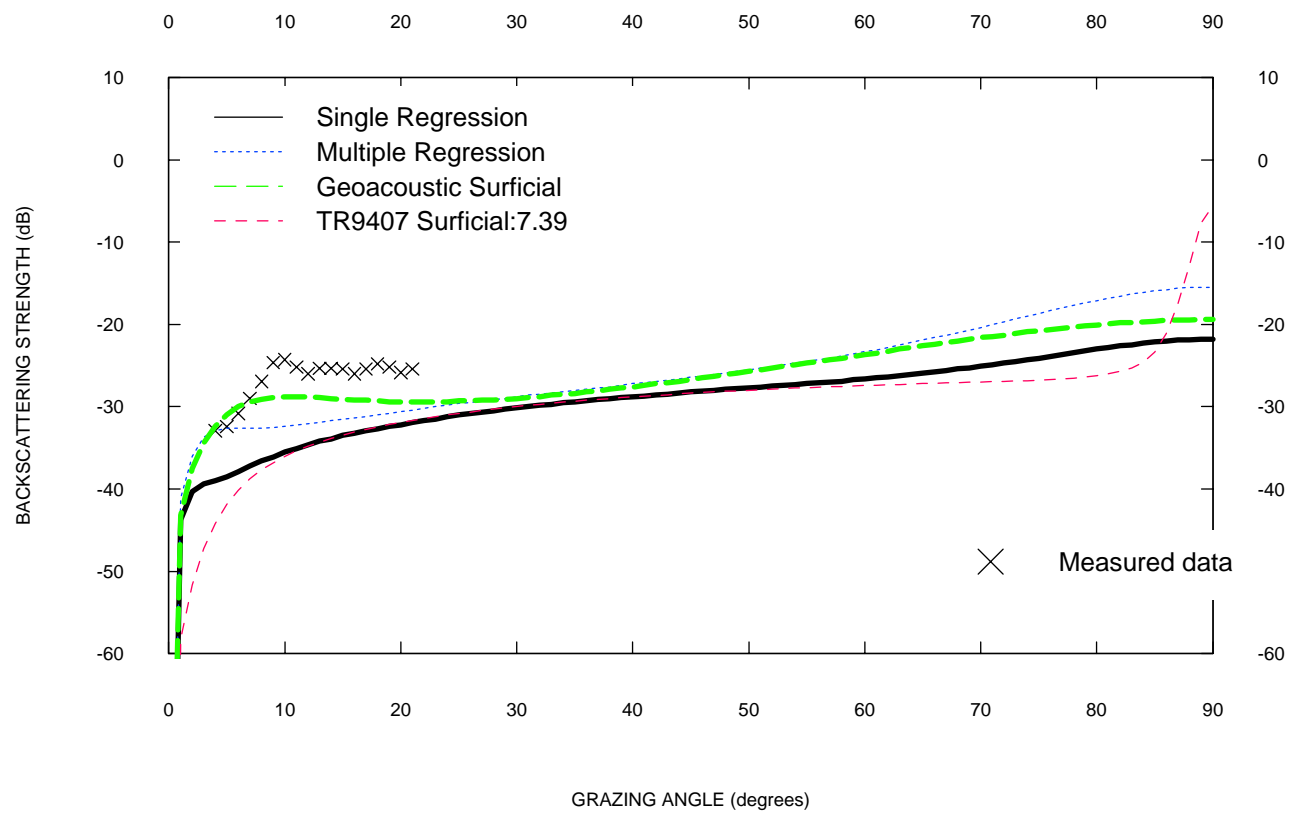
Key_West backscattering at 40 kHz



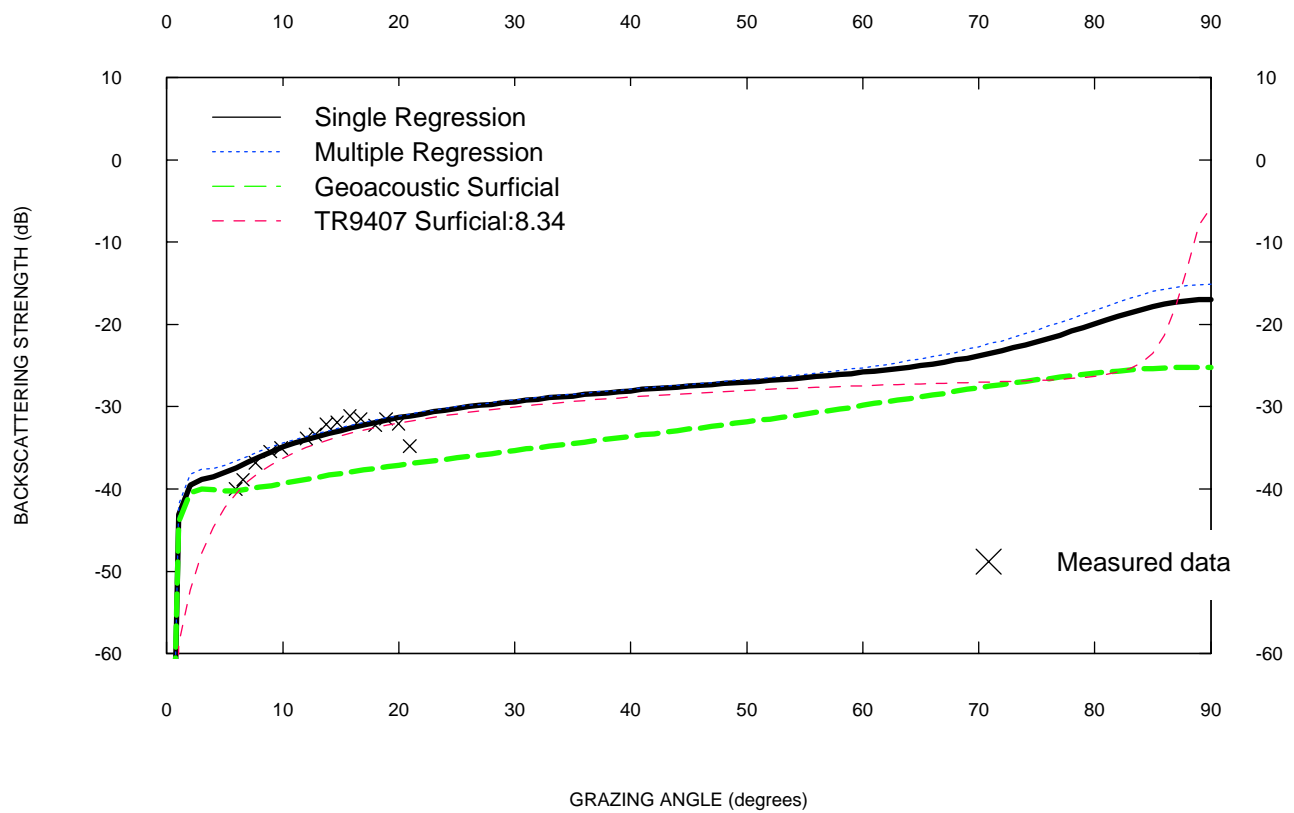
Juan_de_Fuca_Site4 backscattering at 25 kHz



Eel_River backscattering at 40 kHz



Orcas backscattering at 40 kHz



Juan_de_Fuca_Site7 backscattering at 25 kHz

